8-2011

Assessment Of Collimator Jaw Optimization In Reducing Normal Tissue Irradiation With Intensity Modulated Radiation Therapy

Sarah Joy

Assessment of Collimator Jaw Optimization in Reducing Normal Tissue Irradiation

with Intensity Modulated Radiation Therapy

A

THESIS

Presented to the Faculty of

The University of Texas

Health Science Center at Houston

and

The University of Texas

M.D. Anderson Cancer Center

Graduate School of Biomedical Sciences

in Partial Fulfillment

of the Requirements

for the Degree of

MASTER OF SCIENCE

By

Sarah Joy, B.S.

Houston, TX

August, 2011

Acknowledgements

I must first thank my advisor, Dr. Peter Balter for his incredible guidance, patience, and dedication to excellence. I feel greatly benefited from your research direction and quality clinical training, and am very pleased and privileged to have you as my advisor. I would also like to thank my committee, for their ideas and contributions to my work: Dr. George Starkschall, Dr. Stephen Kry, Dr. Mohammed Salehpour, Dr. R. Allen White, and Dr. Steven Lin. I would particularly like to thank Dr. Starkschall for his amazing edits and commitment to teaching the students of this program.

Special thanks must be given to Dr. Bum Choi for his patience and assistance with Pinnacle scripting, and for his composition of the base script for this work. I would also like to thank Dr. Ramesh Tailor for contributing his measured small field collimator scatter factors which helped make this work possible. Dr. Choi and Dr. Tailor generously contributed to this research and I am truly grateful.

Dr. Xin Wang was extremely accommodating with helping and instructing me in all Pinnacle modeling aspects and allowing the exploration of his new model. Many thanks go to the engineers who are always willing to help and answer questions, and are very patient and pleasant.

Finally I would like to thank my classmates and friends for their good humor and support, and for making each learning experience special and fun. I wish you all the best of luck in your endeavors.

Assessment of Collimator Jaw Optimization in Reducing Normal Tissue Irradiation with

Intensity Modulated Radiation Therapy

Sarah Joy, BS

Supervisory Professor: Peter Balter, Ph.D.

Purpose: To evaluate normal tissue dose reduction in step-and-shoot intensity-modulated radiation therapy (IMRT) on the Varian 2100 platform by tracking the multileaf collimator (MLC) apertures with the accelerator jaws.

Methods: Clinical radiation treatment plans for 10 thoracic, 3 pediatric and 3 head and neck patients were converted to plans with the jaws tracking each segment's MLC apertures. Each segment was then renormalized to account for the change in collimator scatter to obtain target coverage within 1% of that in the original plan. The new plans were compared to the original plans in a commercial radiation treatment planning system (TPS). Reduction in normal tissue dose was evaluated in the new plan by using the parameters V5, V10, and V20 in the cumulative dose-volume histogram for the following structures: total lung minus GTV (gross target volume), heart, esophagus, spinal cord, liver, parotids, and brainstem. In order to validate the accuracy of our beam model, MLC transmission measurements were made and compared to those predicted by the TPS.

Results: The greatest change between the original plan and new plan occurred at lower dose levels. The reduction in V20 was never more than 6.3% and was typically less than 1% for all patients. The reduction in V5 was 16.7% maximum and was typically less than 3% for all patients. The variation in normal tissue dose reduction was not predictable, and we found no clear parameters that indicated which patients would benefit most from jaw tracking. Our TPS model of MLC transmission agreed with measurements with absolute transmission

differences of less than 0.1 % and thus uncertainties in the model did not contribute

significantly to the uncertainty in the dose determination.

Conclusion: The amount of dose reduction achieved by collimating the jaws around each

MLC aperture in step-and-shoot IMRT does not appear to be clinically significant.

Table of Contents

List of Figures

List of Tables

List of Equations

1 Introduction

1.1 Statement of Purpose

Of all cancers worldwide, lung cancer is the most prevalent and accounts for the most deaths as of 2008[1]. Chemoradiation therapy has been shown to effectively control the most common type of lung cancer, non-small-cell (NSCLC), but to achieve local control of 90% a dose of 80Gy may be required[2]. Currently prescription doses typically remain at or below 70Gy due to the normal tissue structures surrounding the cancer. In general, the higher the prescription dose to the tumor the higher the probability of inducing a normal tissue toxicity such as lung pneumonitis, esophagitis, or a decrease in pulmonary function.

Intensity Modulated Radiotherapy (IMRT) can provide dose escalation in comparison to 3D conformal radiotherapy (3DCRT) by increasing conformity of the prescribed dose to the target while decreasing normal tissue doses. However, IMRT may still deliver low damaging doses to normal tissues outside of the radiation field due in part to leakage and transmission through the mulitleaf collimators (MLCs)[3, 4]. It is possible these low doses may be reduced on the Varian 2100 platform by moving the jaws to the edge of the MLC aperture for each segment of step-and-shoot IMRT. Currently Varian 2100s allow one jaw position for each beam, limiting clinical practice to jaw collimation of the maximum MLC aperture in each beam. This potential to reduce low doses by jaw tracking each aperture is illustrated in Figure 1.1 with three segments of a step-and-shoot IMRT beam with fixed jaws positions around the

target (red), and then in Figure 1.2, in which the same three segments are shown with the jaw tracking method (JTM), blocking transmission to the esophagus (green), heart (pink) and other normal tissues. This JTM could be used to decrease the probability of a normal tissue toxicity, or be traded off for a higher prescribed dose that could potentially increase local control.
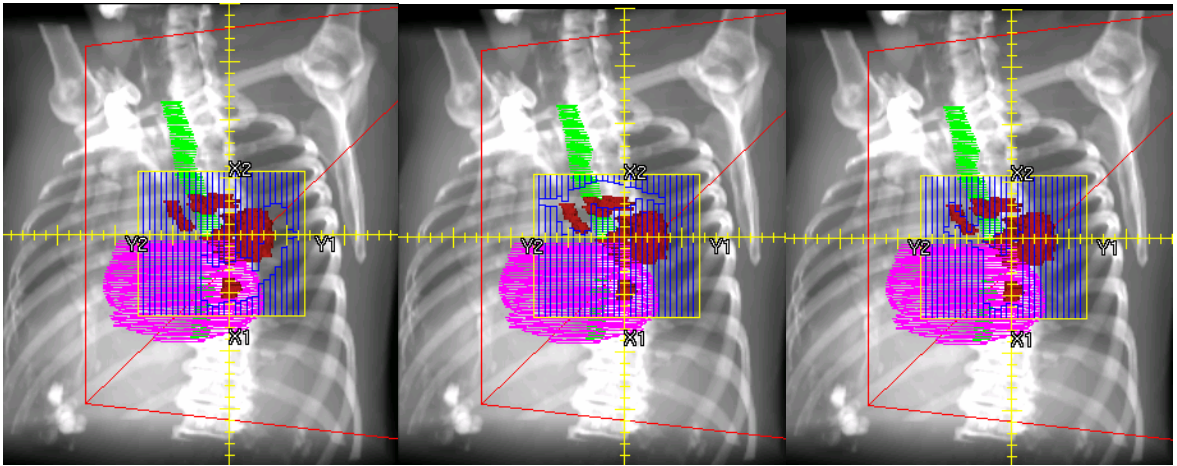
Figure 1.1 Three segments of original step-and-shoot plan
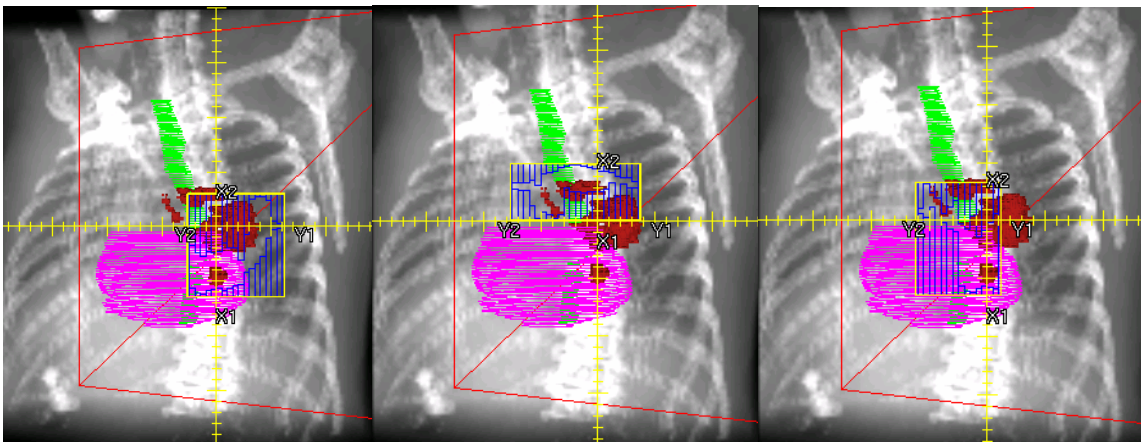
Figure 1.2 Three segments of JTM step-and-shoot plan with jaw tracking

2

1.2   Normal Tissue Toxicities in Thoracic Radiotherapy

Radiation-induced pneumonitis remains the primary concern for most thoracic treatments in which the lung is exposed to the treatment field. Pneumonitis typically occurs three to six months following treatment and is characterized by inflammation of the lung due to irradiation, resulting in decreased gas exchange [5].The degree of toxicity has been defined by many groups but the Southwest Oncology Group (SWOG) scores radiation pneumonitis as the following:

Grade 1: Asymptomatic or symptoms not requiring steroids

Grade 2: Radiographic changes and requiring steroids or diuretics

Grade 3: Radiographic changes and requiring oxygen

Grade 4: Radiographic changes and requiring assisted ventilation

Grade 5: Death

Graham et al. [6]correlated the incidence of pneumonitis as well as grade with the volume of normal lung receiving 20Gy (V20); they found all fatal pneumonitis events to occur when V20>34%. This paper serves as one guideline for evaluating the total normal lung on a dose-volume-histogram (DVH), and shows that V20 should be below 35% but preferably as low as achievable. Mean lung dose has also been correlated with pneumonitis [7, 8], but only with incidence of pneumonitis Grade 2 or higher; incidence of the different grades were not distinguished.

Another toxicity of concern is radiation esophagitis, in which patients have soreness and difficulty swallowing (dysphagia) due to the esophagus inflammation resulting from irradiation. This presents acutely two to three weeks following treatment and may potentially lead to morbidity from weight loss and dehydration. The two main grading systems for toxicity are from the Radiation Therapy Oncology Group (RTOG) and the National Cancer Institute Common Toxicity Criteria (NCI-CTC). The NCI-CTC defines their scale as the following:

Grade 1: Mild dysphagia but can eat regular diet

Grade 2: Dysphagia, requiring predominantly pureed, soft, or liquid diet

Grade 3: Dysphagia, requiring feeding tube, IV hydration, or hyperalimentation

Grade 4: Complete obstruction (cannot swallow saliva); ulceration with bleeding not induced by minor trauma or abrasion or perforation

The RTOG scoring criteria is very similar to the above, with an additional requirement of dehydration or weight loss for Grade 3. The incidence of acute esophagitis for Grade 1 or higher has been correlated with V35 [9, 10], it has also been correlated with V50[11] and V60[12] for Grade 2 or higher toxicity.

Pulmonary function tests are typically done before and after treatment in order to gain a more overall sense of lung response to radiotherapy. Testing pulmonary function may include evaluation of the patient's diffusion capacity for carbon monoxide (DLCO) and the forced expiratory volume the patients exhales into a spirometer in 1 second(FEV). The test of

a patient's DLCO typically involves the patient blowing out enough air to reach the residual volume, then taking a full breath of a gas mixture with a small amount of carbon monoxide. The gas is held in the lungs for about 10 seconds and then exhaled and analyzed to find the amount of carbon monoxide taken up during the breath hold[13]. Pulmonary function remains somewhat difficult to quantify as most patients have impaired function before treatment, and some patients see an improvement in pulmonary function after treatment. If seen, the improvement in function results from the lung tumor shrinking due to irradiation, which allows blood flow through pulmonary vessels that were previously obstructed by the tumor[14, 15].

De Jaeger et al. hypothesized that radiation induces damage to alveolar/capillary membrane and perfusion weighted lung function metrics may better estimate functional outcome[15]. DLCO is not perfusion weighted but may also be an optimal measure as it shows a decrease in function after irradiation and is less reliant on tumor related factors than FEV [16]. A reduction in pulmonary function has been linked to mean lung dose [17] and has also been correlated with low doses (5-20Gy) to the total lung[18, 19].

Heart toxicites are another concern in thoracic radiotherapy and may include pericarditis, cardiac fibrosis, and coronary artery disease. Pericarditis is an irritation or swelling of the pericardium which is a thin double-walled membrane that surrounds the heart; this usually results in chest pain. Cardiac fibrosis is a thickening of the heart valves and loss of flexibility which could lead to heart dysfunction. Coronary artery disease is a narrowing of the blood vessels that supply the heart with blood and oxygen; this could result in a heart attack, heart

failure, chest pain or an arrhythmia. It has been generally accepted since the 1950s that more than 40Gy to the mediastinum poses a risk for cardiac disease[20].

Fibrosis occurs months to years after treatment and may be characterized by reduced flexibility and strength, strictures, and possibly pain. It is typically chronic and progressive in severity and lung fibrosis has shown to be correlated with similar dosimetric parameters as pneumonitis[21].

A correlation has been found between the volume of tissue receiving low doses and the incidence of a secondary cancer, and that low dose volumes are greater for IMRT compared to conventional radiotherapy [22]. The increased low dose volumes from IMRT are due to increased head leakage, monitor units (MUs) and MLC transmission [23, 24]. Integral dose is defined as the total energy absorbed per unit density for a structure, and is calculated as in Equation 1.1.

Equation 1.1 $$IntegralDose_{structure} = \bar{D}_{structure} * V_{structure}$$

Equation 1 gives the integral dose for a structure as the mean dose for the structure multiplied by the volume of the structure; most commonly it is defined over all structures for a patient or for normal tissue, which is taken to be all structures minus the PTV. Integral dose may offer a parameter to judge risk of secondary cancer as it describes mean dose to the

patient overall. It has been shown that IMRT either reduces or keeps the integral dose

constant compared to 3DCRT[25, 26] in part due to a reduction in scattered radiation from

smaller field sizes. It may be that collimating the jaw to each segment could further reduce

integral dose by reducing the head transmission and leakage which would be associated with

a decrease in probability of a secondary cancer.

For the dose-limiting toxicities mentioned, there are other factors to consider when

evaluating a patient for incidence such as age, gender, and whether the patient is a smoker or

on chemotherapy; the dosimetric parameters most related to this work are summarized above

and in section 1.5.

1.3   Intensity Modulated Radiation Therapy (IMRT)

Intensity Modulated Radiation Therapy has become a part of standard of care in many

services today. The idea behind IMRT is to deliver nonuniform fluences to the target to better

shape the dose distribution so that more conformity to the target is achieved. As conformity

improves, normal tissue doses near the target decrease and in turn a higher dose to the target

may be deliverable; therefore IMRT treatments frequently contain escalated doses to the

target compared to 3DCRT.

IMRT planning involves inverse planning, in which the user specifies dose constraints to

important structures in an effort to provide adequate tumor coverage while maintaining

reasonable normal tissue doses. The planning system divides a beam up into segments, each

of which has a different MLC shape and weight, and an iterative optimization outputs a plan based on the input parameters and dose constraints the user selected. The optimization utilizes a cost function which is a measure of the quality of the plan. Often the cost function is the root mean square difference between the desired dose and the realized dose which is iteratively minimized.Once an optimized solution is reached, a beam will have segments of different MLC shape and weights, the composite of which gives a nonuniform fluence pattern [27]. This research focuses on step-and-shoot IMRT which involves several segments or subfields of a beam, each of which have a particular MLC shape; during treatment one segment is formed, radiation is delivered for a certain number of monitor units and then the beam is turned off while the MLC takes the shape of the next segment.

With lung cancer, IMRT has been shown to reduce the risk of pneumonitis while maintaining local control [3, 4, 28]; however with dose escalation in IMRT comes increased transmission through the MLCs which contribute low doses to a larger volume.

1.4   Varian Linear Accelerators

MD Anderson's radiation oncology division largely operates with Varian linear accelerators (linacs) as opposed to Siemens or Elekta linacs. Figure 1.3 shows a typical Varian linac with an inside look at the structure of the head of the machine.
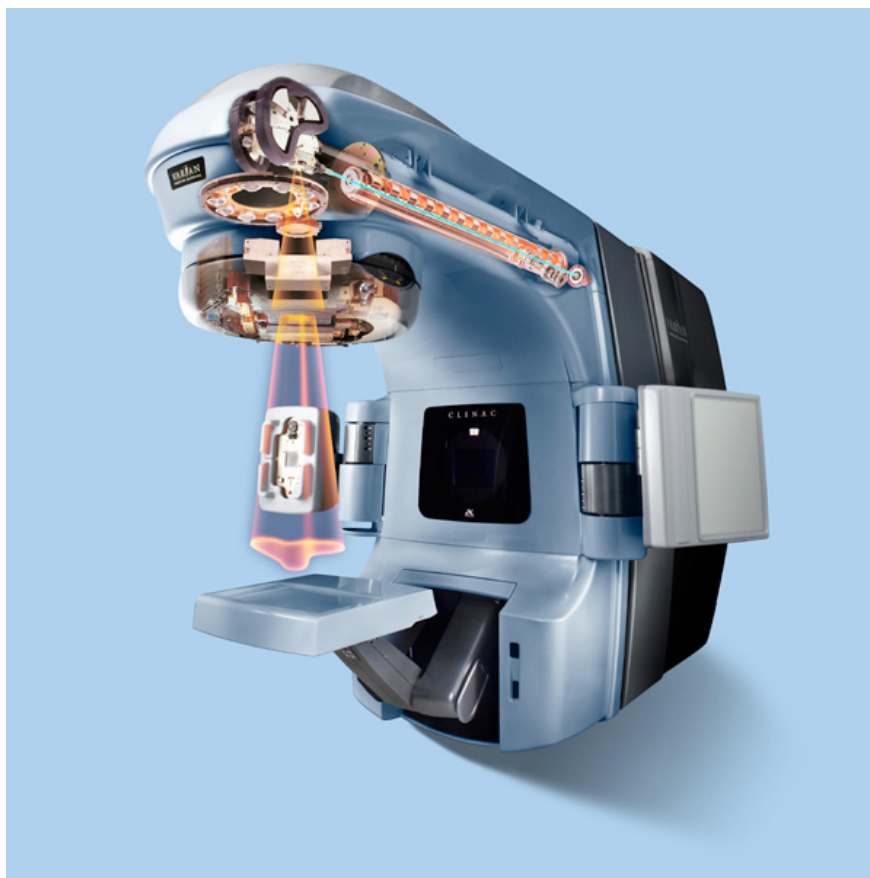
Figure 1.3 Varian 2100 Linac Linear Accelerator

As this project involves using the jaws of the linac to backup the MLCs, it is worth exploring how the construction of the Varian treatment head compares to those in other manufacturer's linear accelerators. Linear accelerators all include a primary collimator located high up in the head of the linac that shapes the beam with appropriate geometry right after the electrons hit the x-ray target or electron scattering foil. After passing through the primary collimator, the beam passes through a flattening filter or electron absorption foil followed by an ionization chamber. After this comes the secondary collimation (movable jaws) which consist of an upper (y-jaws) and a lower set (x-jaws) on Varian accelerators.

9

These thick jaws attenuate 99.9% of the primary beam and move along a curved path to follow the divergence of the beam. Varian machines have MLC banks under the x jaws as a tertiary collimator which allows the addition of MLC capabilities to an existing proven linac. On the downside, this configuration adds bulk and shortens the distance to mechanical isocenter creating longer distances for MLC travel and less clearance space between the linac head and patient. A penalty of this tertiary configuration is increased MLC transmission.

Elekta linacs replace the upper jaws with the MLCs instead of adding them below the lower jaws. Elekta includes a 'backup jaw' which is a thinner jaw which acts only to backup the MLCs. The advantage to this structure is the ability to make a more compact linac head; the MLCs are closer to the source and do not have to travel as far, and therefore can be made smaller. The disadvantage of this configuration is the greater leaf magnification projected at isocenter which requires tighter motion tolerances as well as a large geometric penumbra from the MLC.

Siemens machines replace the lower jaws with MLCs and do not have a backup jaw like the Elekta machines. One major difference between Siemens and other manufacturer's designs is that they have a flat MLC leaf end that is double focused, meaning the MLC ends follow the beam geometry in both the x and y directions. This is different from Elekta and Varian leaf ends, which follow the beam geometry in one direction perpendicular to leaf motion (single focused), and move in a single plane perpendicular to the beam's central axis. Single focused leaves are rounded at the end to decrease the variation in attenuation of the beam with leaf position. Siemens double focused MLCs move in an arc similar to the jaw motion, following a spherical surface centered on the central axis. This allows greater leaf position accuracy and narrower penumbra but is more difficult to control and design

mechanically[29, 30]. As Siemens and Elekta both use the MLC in replacement of a jaw, the collimator output factor is determined by the jaw and the MLC whereas in Varian, the collimator output factor is determined by both the upper and lower jaws and not by the MLC.

1.5   Low Doses in Thoracic Cancers

Though typical dosimetric parameters related to normal tissue toxicities in thoracic cancers may be at relatively high doses, some recent research has led to concern over lower doses also inducing toxicities. The low dose range studied was from 0-20Gy over a large volume, the parameters looked at include the volumes of heart and lung doses receiving a particular low dose.

Taylor, et al reviewed cardiac disease for breast cancer patients and indicated an increased risk of heart toxicity from radiation therapy for those patients whose heart volume receiving between 0 and 5Gy was large[31].

Two studies looking at treatment related pneumonitis also found results indicating that the volume of normal lung receiving 5Gy was significantly correlated to occurrence of this toxicity. One paper [32] looked at non-small cell lung cancer (NSCLC) patients who underwent 3DCRT concurrently with chemotherapy; those who had pneumonitis that needed oxygen (Grade 3 according to the scale listed) or worse were correlated with clinical and dosimetric parameters. It was found that relative volume of normal lung, that being total lung minus GTV (gross tumor volume), getting 5Gy was associated with an increased risk of developing pneumonitis. Patients with V5 less than or equal to 42% were significantly less likely to have an incidence that was Grade 3 or higher. The other study focused on IMRT plans for mesothelioma patients who had extrapleural pneumonectomies and found a 10%

incidence of pneumonitis for patients with a mean lung dose of less than or equal to 15Gy. It was also found that most patients who developed pneumonitis had a V5 above 81% but had V20 less than 20%. V5 was investigated for prior patients and the majority of them had a V5 of greater than 90%; it was suggested this parameter may have been largely contributing to pulmonary toxicity seen with those patients[19]. The overall results of these two studies indicate that V5 may predict incidence of radiation pneumonitis.

Gopal [18] analyzed pulmonary toxicity in NSCLC patients undergoing concurrent chemoradiation with amifostine and found a sharp decrease in diffusion capacity at a dose of 13Gy.

Lee et al [33] found a correlation between pulmonary complications in esophageal patients treated with chemoradiation, and irradiating greater than 40% of lung volume with 10Gy.

In the way of thoracic cancers, low doses may be more harmful than previously thought and volume constraints on these doses would benefit thoracic patients.

1.6   Jaw Collimation to MLC Aperture

The amount of normal tissue dose reduction from backing up the MLC with the jaw is uncertain for clinical plans. Some work has been done looking at the differences between dosimetric parameters for fields defined by the jaws only, MLC only and combined MLC and jaw. Kehwar et al. [34] measured the PDD (percent depth dose) curves, cross plane profiles and dose rate for each of the fields mentioned above and found that the dose rate in air was higher for MLC and jaw for 6MV and higher for MLC only for 15MV and there was

little difference between the MLC and jaw field and the jaw only field. For PDDs the surface dose and buildup was decreased for MLC and jaw fields compared to MLC only and jaw only fields, and there was no significant difference between the MLC only, jaw only and MLC and jaw fields for profiles and penumbra. This work was done with a Varian Millenium 80-leaf system. A similar study [35]done with a Varian 120–leaf system found that dose rate was higher in a solid water phantom for the MLC only field and that there was no significant difference in dose rate between the MLC and jaw field and jaw only field. The surface and buildup dose was also higher for the MLC only field with no significant difference in the PDD beyond the depth of maximum dose (dmax). The profile width and penumbra were larger for the MLC only field.

Another study [36]looked at dose at dmax for different MLC field sizes each with various jaw sizes, all normalized to dose at dmax for a 10x10 field set by the jaws; the maximum change in output was 5% and occurred when the jaws were at their maximum field size and the MLCs were at their smallest size.

These studies give an idea of the benefit that could be wrought from using fields with the jaws pulled in close to the MLC, but they don't apply directly to treatment plans. Tobler et al [37] used the BrainLAB treatment planning system to compare dose profiles for fields whose jaw sizes were at their maximum setting to those at smaller field sizes. The profiles for the larger field sizes extend out to further off-axis distances and show a higher amount of dose getting through for the same micro-multileaf collimator field size. The percent volume covered by different isodose levels for single isocenter patient plans were compared for plans with jaws at the maximum setting to plans with the jaws brought in flush with the micro-MLC tips for each field. For the patient with the smallest field defined by the micro-MLCs,

the maximum difference occurred for the smaller isodose levels, up to 60% difference in the volume covered. Another paper found less of an improvement with three prostate patient plans looking at differences between a jaw setting 5mm outside the MLC in the x-direction and 3mm outside the MLC in the y direction, and one that is optimized the cover the rectal wall with the collimator angle changed from 180 degrees and jaws pulled in flush with the edge of the MLC tips. The study found the volume of rectal wall receiving 60Gy had a 3%, 4.7% and 9.6% reduction with the jaw optimization[38].

Schmidhalter et al [39]explored the possibility of collimating the MLC aperture with the jaws for dynamic academic and clinical cases. For clinical cases they chose a prostate and head and neck plan and only brought in the x jaws with a 5mm margin from the edge of the most open MLC. The prostate plan was a five field IMRT plan and measurements were taken with film for 6 and 15MV at a depth of 5cm in a solid water phantom at 100cm SSD (source to surface distance) and a gantry angle of zero degrees. The head and neck plan had the same parameters and measurements except it was an eight field plan. Gamma analysis was done on all films using 3%/3mm criteria[40] and all values were less than 1. For the prostate plan the volume body minus PTV was reduced by 1.7% with the optimized jaw plan with the total MU increased by 2.6% for coverage. The head and neck plan volume body minus PTV was reduced by about 1.5% and the total MU increased 2.8%. Both plans had a small decrease in doses to some of the organs at risk, the largest difference being in the head and neck plan, 7% decrease in the DVH of myelon.

1.7   Hypothesis and Specific Aims

Closing the jaws of the linear accelerator in around the MLC aperture for each segment of step-and-shoot IMRT could provide a decrease in the larger volumes of normal tissues receiving low doses; but the question of whether the volumes receiving low doses could be reduced significantly by using this method remains unanswered.

The hypothesis of this study was: *The volume of lung receiving 20 Gy can be reduced by greater than 10% by using the linac jaws to tightly collimate each aperture of the MLC in step-and-shoot IMRT.*

The specific aims of this study were:

- To determine a method of implementing tight collimation around the MLC aperture on a segment-by-segment basis in the treatment planning system and in treatment delivery.

- To select thoracic patients undergoing radiotherapy using step-and-shoot IMRT and modify the clinical plan to have the jaws track each segment and compare the calculated doses between the clinical and jaw plans.

-To verify the accuracy of the treatment planning system by measuring MLC and jaw transmission and comparing to calculations.

2 Materials and Methods

2.1 Varian MLC Characteristics

The MLC system used for this project has 120 leaves (Millennium 120, Varian Associates, Pala Alto, CA) which includes 60 pairs of tungsten leaves. The leaf dimensions given here are all optical projections at isocenter, where the distance from the center of the leaf to isocenter is approximately 49cm. The leaf widths for the first and last leaf pairs are 1.4cm, widths for the second through tenth pairs and the fifty first through fifty ninth pairs are 1cm, and all the central pairs are 0.5cm in width. The leaves sit on a carriage split into two banks each holding 60 leaves; the carriage can move the MLCs linearly or rotate them. The most a leaf can extend beyond the most retracted leaf is 15cm; if the field is larger than that, options are to split the field or to linearly move the MLC carriage. The leaf effective shielding length is 15cm and the average transmission across all leaves is about 2% with interleaf transmission peaks of 2-3%, about 1% additional interleaf transmission. The transmission with the jaws backing the leaves should be less than 0.5% according to the manufacturer [41]; as low as 0.1% transmission has been measured [42].

MLC transmission may vary slightly under different sections of the MLC; most commonly the average is taken, but to be more accurate both intraleaf and interleaf transmission values may be given. Intraleaf transmission refers to photons passing through the entire height of the leaf while interleaf transmission refers to photons passing between leaves, through the tongue and groove (Figure 2.1). The tongue and groove is meant to reduce interleaf transmission by providing some attenuation at each point between leaves. LoSasso has reported MLC transmission values between 1.7 and 2.7%, the latter being

interleaf transmission, consistent with Varian's specifications and measurements done at MD
Anderson.
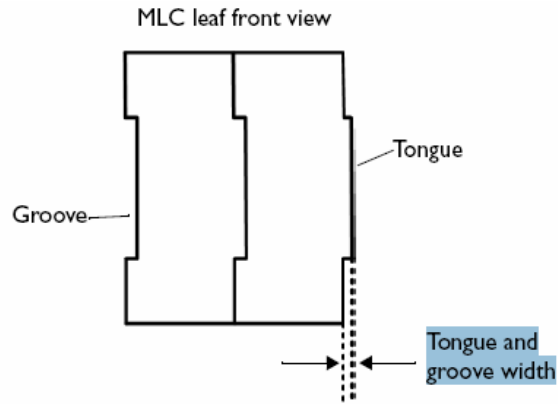
Figure 2.1 Tongue and groove width model

Leaf end penumbra was studied and the added transmission due to the rounded end was
found to be equivalent to increasing the field size of a focused collimator by 1mm on each
side[43]. Varian has two correction files to correct leaf positions, one generic to all
Millennium MLC and the other has the following adjustable parameters: skewness of each
leaf bank, gap width and centerline offset. Skewness of the MLC carriage refers to how
shifted the MLCs are from alignment with the jaw. Centerline offset refers to the carriage's
distance from the central axis; both MLC banks should be symmetrical about the central axis.
The gap width refers to the nonzero opening between closed leaves which prevents leaf
collision. Gap width for the central leaves was found to be slightly larger than that for the
peripheral when measured with a feeler gage for several Varian linacs with no clear reason
why, while it was found that transmission varies with gantry angle only minimally [43].

2.2 Pinnacle Collimation Modeling

The commercial radiation treatment planning system (Pinnacle[3], v *m.n*, Philips Medical Systems, Milpitsa CA) models the rounded leaf end as a circle with a radius that outlines the leaf end and that has a center near the center of the leaf (Figure 2.2); the typical radius for Varian machines is 8cm[44]. Pinnacle uses this model to compute the differential attenuation determined by the thickness of the leaf end along each ray line.
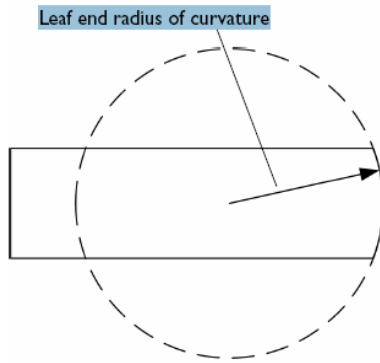
Figure 2.2 Pinnacle model of rounded leaf end

The tongue and groove effect is modeled by entering a width of the tongue and groove that most closely matches the measured profiles; Figure 2.1 shows the tongue and groove for two MLCs and the defined width. The tongue and groove tries to minimize leakage between leaves but the overall thickness the beam goes through is reduced from the leaf thickness, leading to about 1% higher interleaf than intraleaf transmission. In Pinnacle, the user may add a value for this additional interleaf leakage to the average MLC transmission value; the system does not take into account increased measured transmission with increased field size. [45]

2.3 Patients

We evaluated plans for 10 thoracic, 3 head and neck, and 3 pediatric patients. All patients in this study were enrolled in an institutional review board-approved retrospective data collection protocol (2005-0574).Thoracic patients were evaluated as low doses to the lung are a justification against IMRT, head and neck plans were evaluated due to the high level of modulation, and pediatric plans were evaluated for potential reduction in integral dose as this may reduce secondary malignancies. Patients who had relatively large treatment volumes were chosen with the idea that more normal tissue would be collimated by the jaws when pulled in to the MLC aperture. The clinically used plan for each patient was taken to be the original plan and every plan used 6 MV photons only. The Jaw Tracking Method (JTM) was implemented for each patient in a new plan. Table 2.1 summarizes some of the patient parameters and the following 16 pictures (Figures 2.3-2.18) of each patient are to give an idea of the shape and size of the target. All original jaw positions are listed as (X, Y) per beam.

Patient	Area treated	Original segments/beam	Total original segments	Total beams in JTM plan
Thoracic 1	Distal esophagus	(8,9,7,9,6,6,8,7)	60	86
Original Jaw Positions (X,Y) (15, 18.2)(14.3,18)(13.2,17.9)(16.1,14.9)(15.5,19)(16.1,18.9)(16.1,18.8)(15.3,18.5)				
Thoracic 2	Hila+mediastinum	(10,9,7,10,11,12,11)	70	76

Original Jaw Positions (10.3,11.1)(9.5,11.2)(9.9,11.1)(10.3,11)(10.9,10.7)(10.3,10.6)(11.1,11)				
Thoracic 3	Bronchus/lung	(10,11,11,11,8,8)	59	92
Original Jaw Positions (14.4,14.4)(13.1,15.9)(13.4,16.8)(13.6,16.6)(14.1,16.6)(14.7,16.6)				
Thoracic 4	Middistal esophagus	(10,9,8,8,10,9,7,9,10)	80	104
Original Jaw Positions (12.8,21.7)(12.5,22)(12.6,16.9)(15.4,21.5)(12.3,10.9)(13,10.8)(15.4,21.4)(14.5,21.6)(12.9,12.8)				
Thoracic 5	Mediastinum/lung	(12,14,7,12,12,14)	71	75
Original Jaw Positions (13,10)(12.5,10.5)(10.5,10.5)(10,10.5)(12,10)(13.5,9.5)				
Thoracic 6	Hilum/mediastinum	(13,11,13,14,12,14)	77	105
Original Jaw Positions (10.5,15)(12.5,18.5)(12.5,14.5)(12.5,17.5)(12,19)(10.5,13)				
Thoracic 7	Lung/mediastinum	(8,8,9,8,8,9,9,8,7,6,6)	86	97
Original Jaw Positions (11.2,11)(12.7,11.5)(13.5,12)(15,12)(12.7,11.5)(12.4,12)(12.3,12)(14,12)(11.5,12.5)(12.1,14)(10.5,12.5)				
Thoracic 8	Esophagus	(12,15,12,11,9,11)	70	83
Original Jaw Positions (13.5,16.5)(12.5,16.5)(11,16.5)(13,16.5)(14,16.5)(14,16.5)				
Thoracic 9	Hilar mass+nodes	(7,6,3,3,4,5,8,10,8,7,9)	70	97
Original Jaw Positions (9,16.8)(9,8.2)(9.3,8.5)(9.4,8.3)(9.8,8.2)(9.5,8.4)(9.7,14.8)(9.8,15.5)(10,12.9)(9.2,16.8)(10.9,13.4)				
Thoracic 10	Mediastinal nodes	(7,11,12,16,11,7,10,8)	82	105
Original Jaw Positions				

(8.9,12.8)(9.3,13.4)(8.2,12.9)(8,10.5)(8.1,10.2)(9.1,11.3)(8.9,12.9)(8.6,13.4)				
HN 1	Oral tongue bed	(12,11,11,11,11,11,11,10,11)	100+3static beams	154+3static
Original Jaw Positions (10,18.4)(10,18.4)(10,18.6)(10,18.3)(10,17.8)(10,19.9)(10,18.2)(10,18.6)(10,18.3)				
HN 2	Base of tongue	(9,10,11,13,10,11,8,10,10)	92+3static beams	131+3 static
Original Jaw Positions (10.6,12)(10.8,12)(11,14)(11,12.8)(11,11.9)(11,13.1)(10.8,12.8)(10.5,13)(10.3,11.9)				
HN 3	Tonsil	(11,12,8,11,12,10,8,12,10)	94+4 static beams	146+4 static
Original Jaw Positions (11,15)(11,17)(11,16.5)(11,15)(11,14.5)(11,16.5)(11,17)(11,15.5)(11,15)				
Pediatric 1	Lung	(9,7,7,7,6,3,9)	48	70
Original Jaw Positions (16.4,15.6)(16.5,15.5)(16.5,14.8)(16.5,14.3)(16.3,13.5)(15.9,13.9)(15.4,15.2)				
Pediatric 2	Liver metastasis	(11,9,8,9,13,10)	60	86
Original Jaw Positions (14,14.7)(15,14.7)(17.8,14.6)(20.8,14.5)(20.5,14.4)(18.2,14.2)				
Pediatric 3	Adrenal Abdomen	(8,15,11,9,8,9,10)	70	79
Original Jaw Positions (9.2,11.5)(8.9,11.4)(10.3,11.3)(10.8,11.3)(9.6,11.3)(10.1,11.5)(9.9,12.8)				

Table 2.1 Patient Parameters

Figure 2.3 Patient Thoracic 1 with target in blue and original isodose lines

Figure 2.4 Patient Thoracic 2 with target in blue and original isodose lines
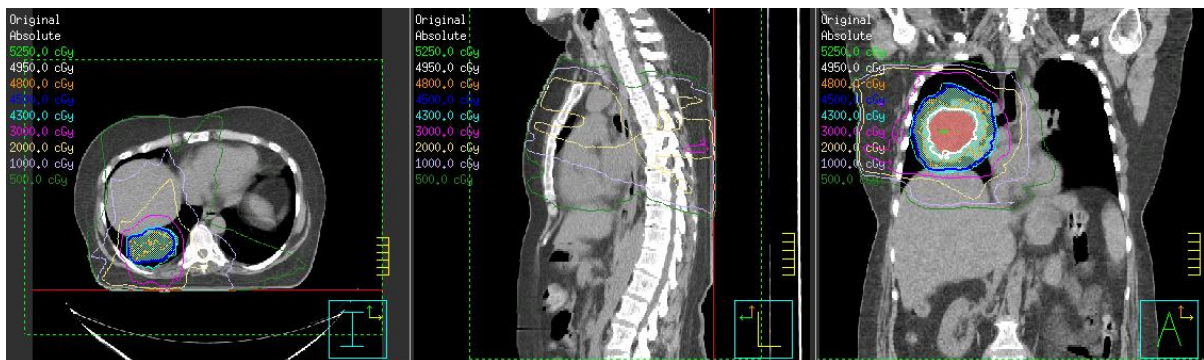
Figure 2.5 Patient Thoracic 3 with target in pink and original isodose lines

Figure 2.6 Patient Thoracic 4 with the target in blue and original isodose lines

Figure 2.7 Patient Thoracic 5 with the target in blue and original isodose lines

Figure 2.8 Patient Thoracic 6 with target in blue and original isodose lines
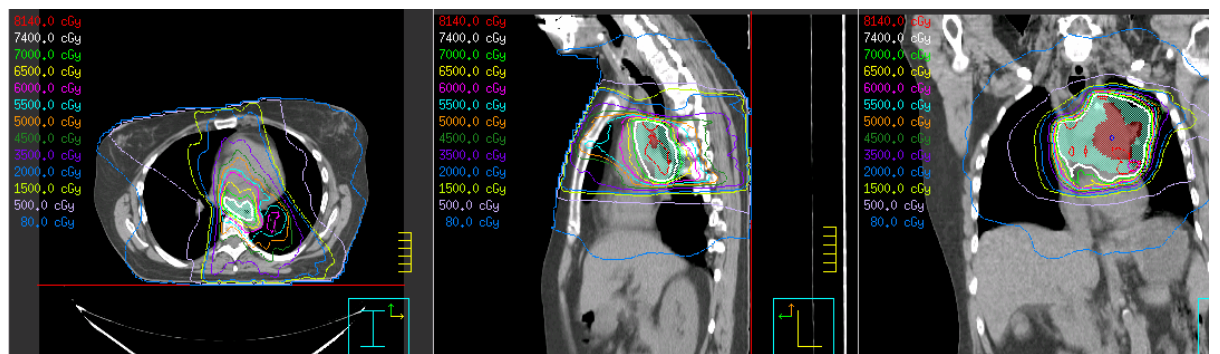
Figure 2.9 Patient Thoracic 7 with target in blue and original isodose lines
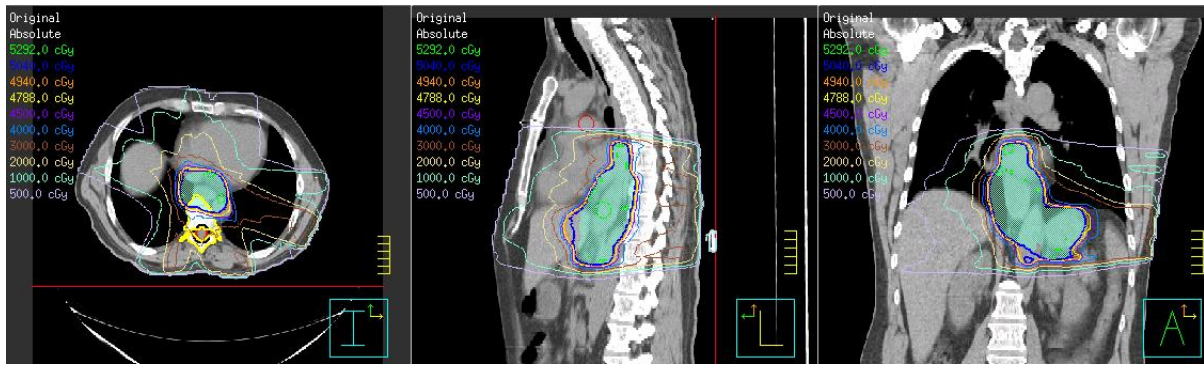
Figure 2.10 Patient Thoracic 8 with target in blue and original isodose lines
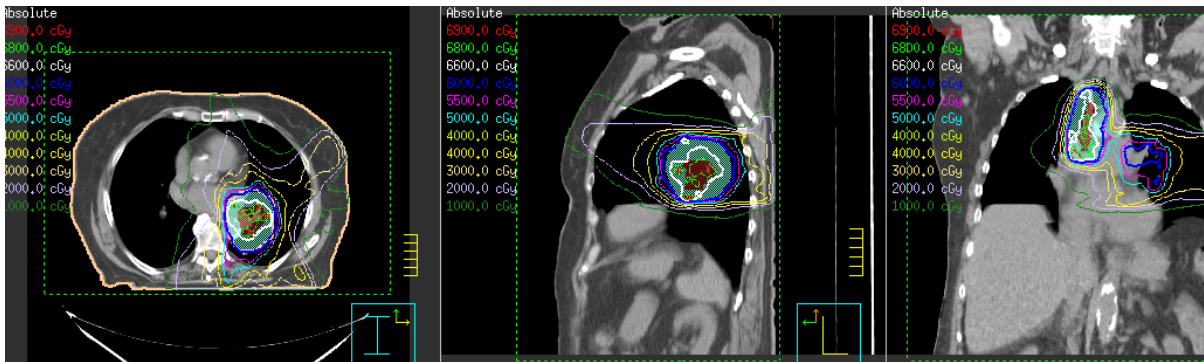
Figure 2.11 Patient Thoracic 9 with target in blue and original isodose lines
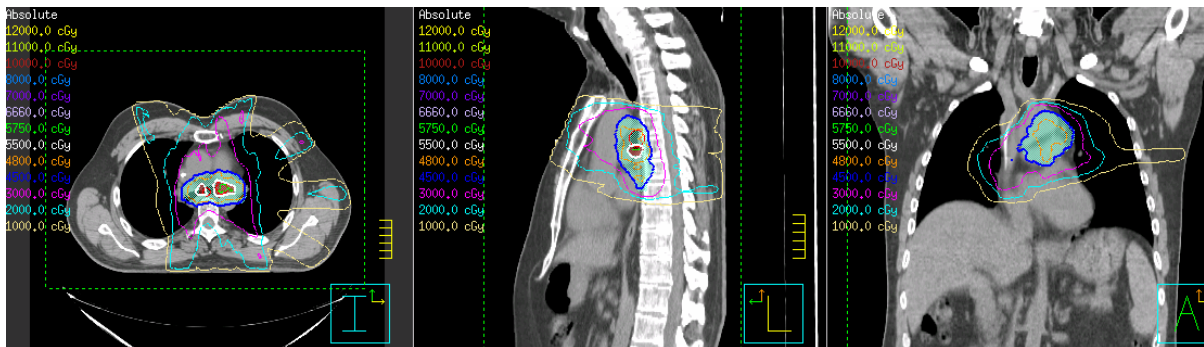
Figure 2.12 Patient Thoracic 10 with target in blue and original isodose lines

Figure 2.13 Patient Head and Neck 1 with target in red and blue and the original

isodose lines
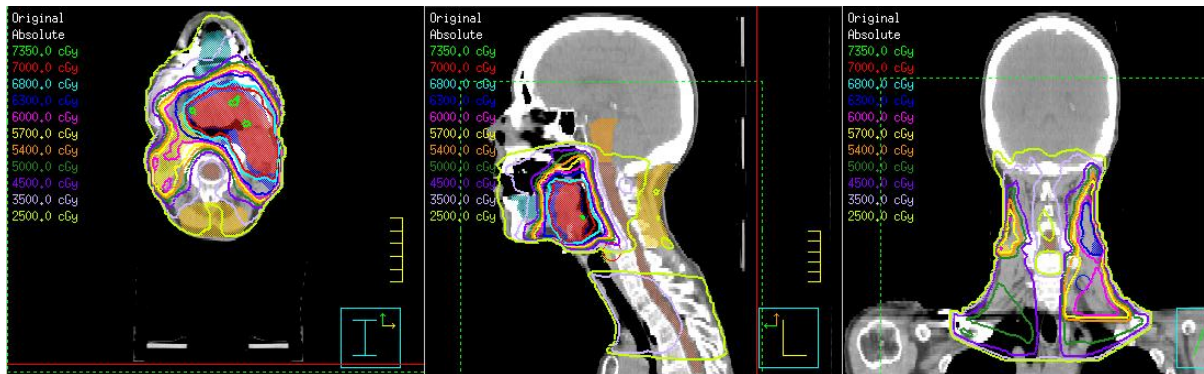
Figure 2.14 Patient Head and Neck 2 with the target in red and the original isodose
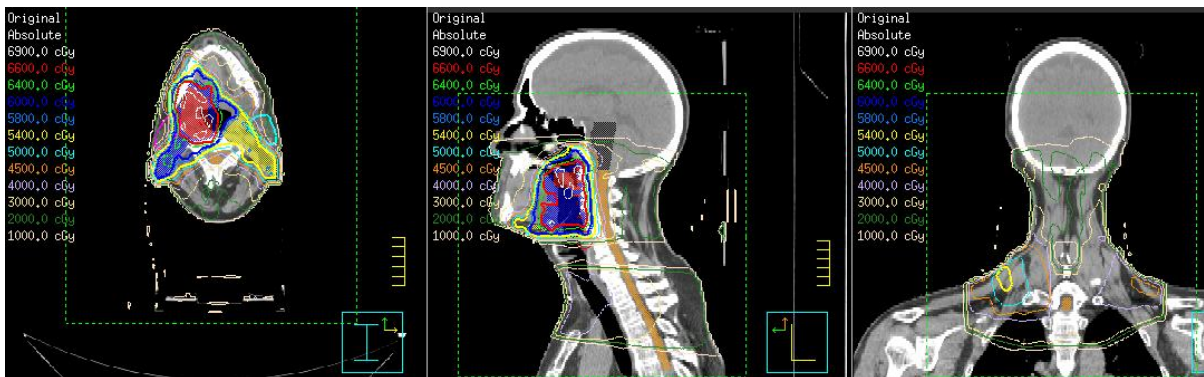
lines

Figure 2.15 Patient Head and Neck 3 with target in red and original isodose lines
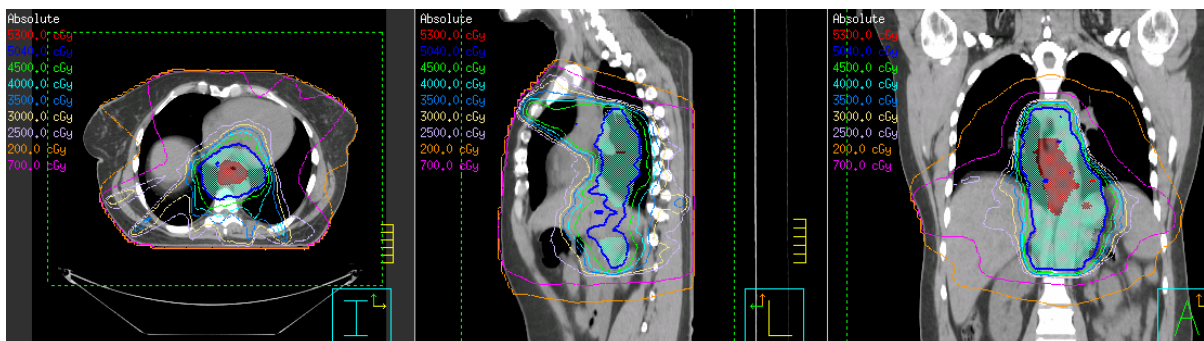
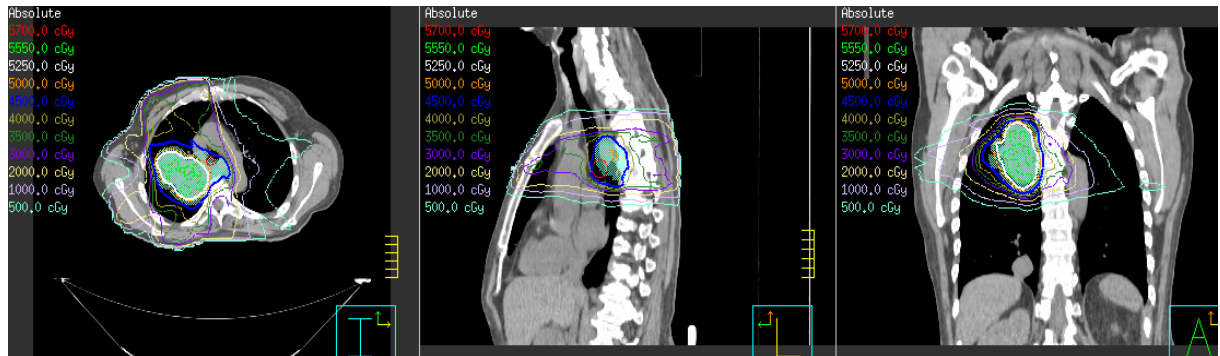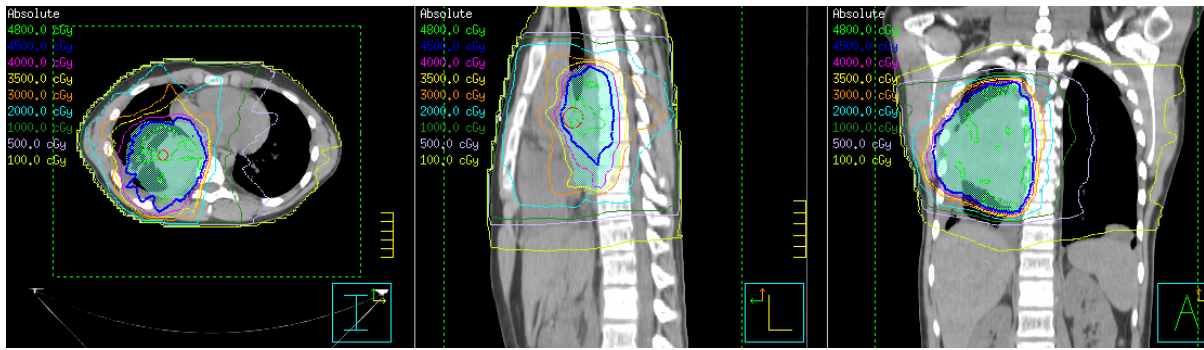**Figure 2.16 Patient Pediatric 1 with target in blue and original isodose lines**
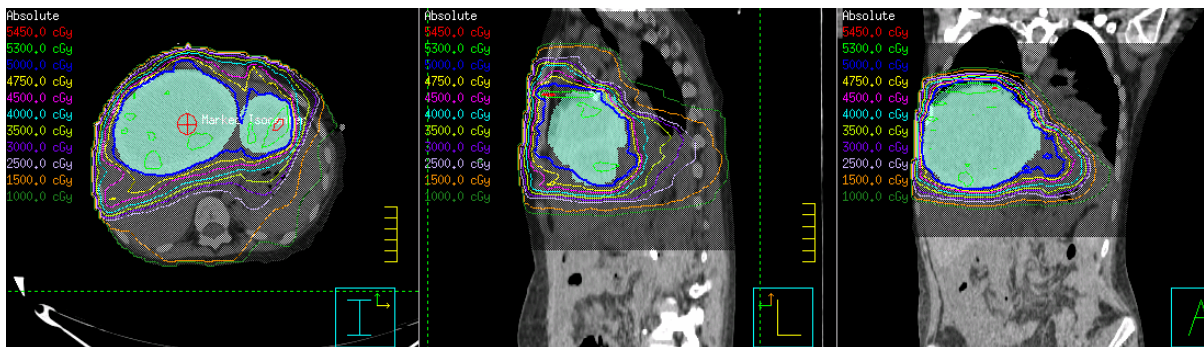
Figure 2.17 Patient Pediatric 2 with target in blue and original isodose lines
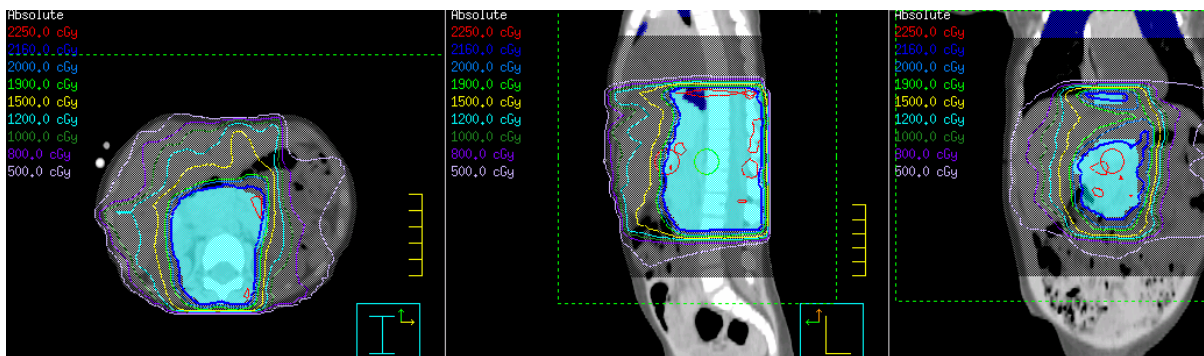
Figure 2.18 Patient Pediatric 3 with target in blue and original isodose lines

2.4   Treatment Plans

In order to create the JTM plan, each patient was moved to our research Pinnacle system. Pinnacle is organized into patients, plans and trials; each patient may have more than one plan and each plan has one or more trials. The trials within each plan share CT datasets and contours but not beams or prescriptions, allowing the user to strive for a better dose distribution with the ability to retain the original and easily compare various trials. For this reason a second trial was created in the patient's clinical plan to implement jaw tracking. It should be noted that each trial in Pinnacle is actually a different treatment plan and we will refer to trials as plans throughout this document. During the process of acquiring patient plans, an upgrade to version 9 of Pinnacle took place and as a result some patients were originally planned in version 8, however all JTM and original (clinical) plans were calculated using version 9 for proper comparison though there should be no difference between the collapsed cone convolution for each version[46]. We also created a special Pinnacle model of the Varian 2100 to accommodate our JTM plan's small fields by adding collimator scatter factors below 4 cm^2; the scatter factors for larger fields remained the same for original and JTM plans. These small field collimator scatter factors were measured by an MD Anderson physicist as part of an ongoing project exploring small field parameters, using a 0.01cc ion chamber with brass buildup[47].

Creating the JTM plan began with copying each original beam once for each control point (segment) in that beam. For example if there were six beams in the original plan and each had five control points then there would be 30 beams in the JTM plan for that original beam. Control points were then deleted so that each beam represented one of the original control points. For example, if beam one of the original plan had five control points then beams one

27

through five of the JTM plan each represent those control points and their respective MLC shapes.

The process of converting the original beams with segments into a beam per segment was done using Pinnacle scripting. Pinnacle scripts were also used to generate ASCII files of the original jaw positions and MUs per control point. Once there was a beam in the JTM plan for each control point, the treatment plan was exported as a DICOM (Digital Imaging and Communications in Medicine) file into MATLAB and a script was used to create a new file with locations of each beam's MLC positions. This file was then called in another MATLAB script that sorted each beam's MLC positions and put them each into an array that mimicked the way Pinnacle presents them. When viewing the MLC positions in Pinnacle, there are two columns with a left (X1) and a right (X2) bank of 60 pairs of leaves, with the cell giving the X position and a leftmost column indicating which leaf pair has that X position. This information is given as if looking from the Beam's Eye View (BEV) with the collimator at zero degrees.

Each set of MLC positions was then written to a file for the variable 'MLC' which included all the beam's MLC positions. This file was imported into another script to find which beams have multiple apertures; in order to fully employ jaw tracking, copies of beams with multiple apertures were made so that each beam in the JTM plan corresponds to one MLC aperture in the original plan. The beams with multiple apertures found were copied in Pinnacle and MLC positions were changed so that only one aperture would exist per beam. These copied beams were recorded to identify which segments of the original plan had copies. Figure 2.19 shows one beam in the original clinical plan with multiple apertures and

Figure 2.20 shows the resulting three beams in the JTM plan, each with one aperture from Figure 2.19.
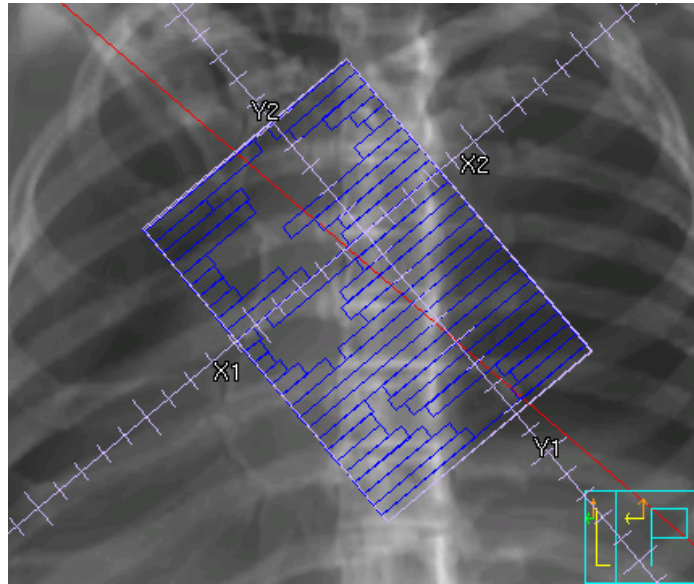
Figure 2.19 Original segment with three apertures: beam 2 control point 1
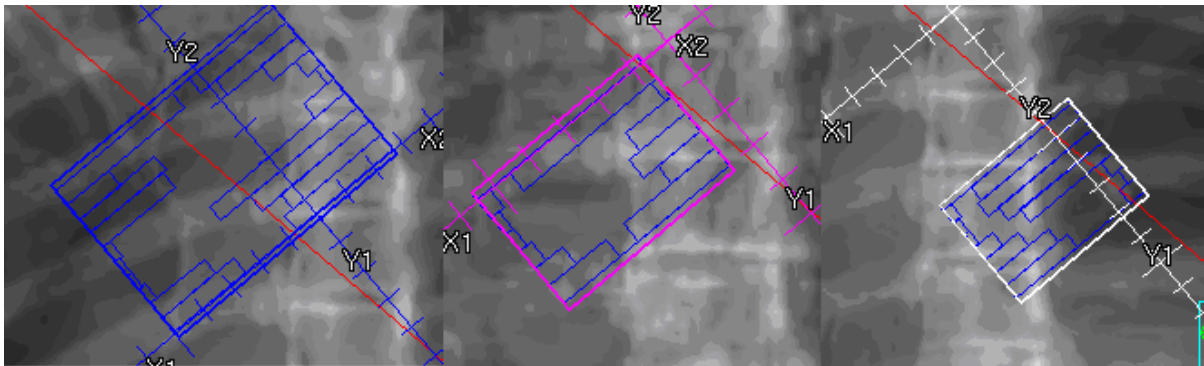
Figure 2.20 JTM plan with beam 8, beam 84 and beam 103 each with one MLC

aperture with jaws pulled in

The DICOM file was exported again for the new MLC positions and the process was repeated with the exception of the last script that finds MLC apertures. There were two

MATLAB scripts to find the new jaw positions for each beam based on the MLC positions; one yields each beam's jaw position by finding the most open leaf in each direction and adding 2mm, and the other script writes this to a file that is in Pinnacle script language. This file was then transferred to a Pinnacle script and ran so that each beam's X and Y jaws were pulled 2mm outside the edge of each aperture. The 2mm margin was chosen because the maximum uncertainty in jaw position is 1mm and in each leaf position is 0.1mm, so this total uncertainty was rounded up for ease of practice. Each beam was visually verified to have jaw collimation of 2mm.

We determined the MU for each beam in the JTM plan by taking the MU for the corresponding segment from the original plan and rescaling it by the ratio of the collimator scatter factor (Sc) for the original plan to that of the JTM plan based on the original and new jaw sizes (Equation 2.1).This was done to maintain the original weighting per segment however due to uncertainties in the Sc, this was not adequate and another renormalization was applied to maintain target coverage.

$$MU^{new}_{ControlPoint} = \frac{S_C^{old}}{S_C^{new}} * MU^{old}_{ControlPoint}$$

Equation 2.1

For copied beams from multiple aperture segments, the monitor units of the original beam containing all the apertures were applied in Equation 2. The ratio of their scatter factors differed because the new jaw positions were different for each aperture, so each beam's final MUs for that one original segment is different.

A MATLAB script performed the monitor unit scaling by first importing the jaw sizes for the JTM and original plans and the MUs. The equivalent square was found for all the jaw sizes and used to interpolate a Sc value. The new MUs for each beam were written to a file as

a Pinnacle script, then inserted into a Pinnacle script to assign the proper monitor units to each beam.

The collapsed cone convolution[48] was used as the dose algorithm for both JTM and original plans and the prescription in the JTM plans were changed to total MUs as opposed to Gray per fraction in order to match the assigned Mus. Decimal monitor units were also allowed in our Pinnacle model in an effort to be as accurate with the scaling as possible; however this cannot be delivered through the standard Varian interface without the Varian Research Toolbox. After rescaling the MUs, the target coverage was still insufficient so the prescription was renormalized to deliver a dose within 1% of the original plan. Figure 2.21 demonstrates the overall process in converting original clinical plans to JTM plans.
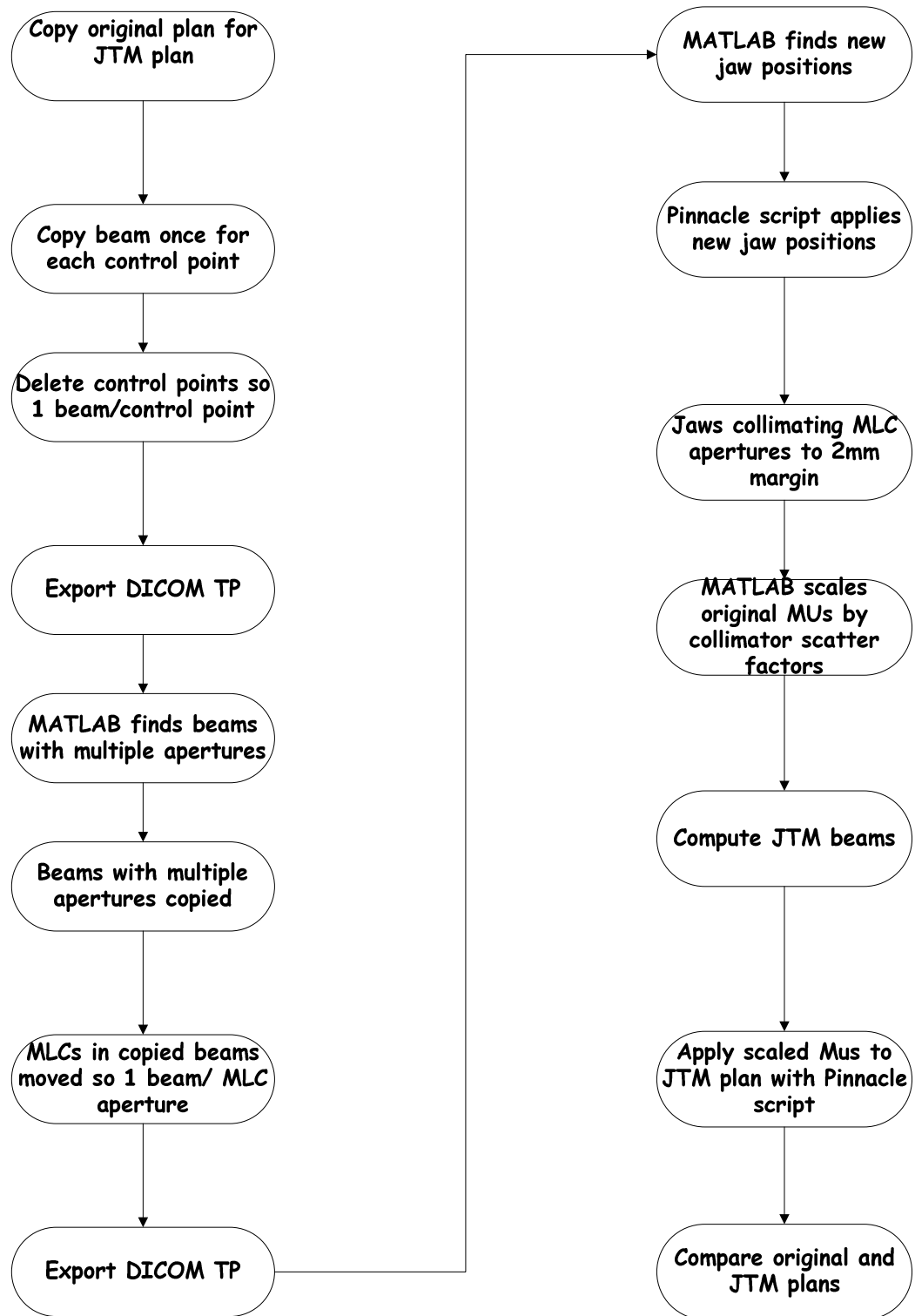
Figure 2.21 Flowchart of process of converting original plan to JTM plan

2.5   Off axis-output factors

The uncertainty in our Sc may be from our use of central axis measurements; many fields are off axis and this was not taken into account in our scaling and therefore may explain our need to renormalize further. We investigated this effect by calculating off axis output factors in Pinnacle for field sizes 2x2, 3x3, 5x5 and 8x8 by normalizing the dose at off axis points to a dose for 10x10 on central axis, then dividing out the off axis factor. Equation 2.2 demonstrates this for a field size a x b at a distance r off axis.

$$\textbf{Equation 2.2} \qquad \frac{D_{axb}(r)}{D_{10x10}(cax)OAF(r)}$$

2.6   MLC and Jaw Transmission Measurements

Measurements of MLC transmission were performed to validate the accuracy of Pinnacle's modeling. Calculations were first executed in Pinnacle then measurements were carried out on a Varian 2100 linac. In Pinnacle, a numerically created water phantom was used as the planning CT dataset and two regions of interest (ROI) were placed within it on the central axis to simulate the 0.6cc ion chamber used; one at 1.5cm (dmax) and 5 cm depth. A density override was also performed on the entire water phantom to change from water to polymethyl methacrylate PMMA which was actually used for measurements. Six beams were made, three of them open fields of sizes 5x5, 10x10 and 12x12 and the other three with the

33

jaws at the same position but with the MLC covering the beam opening. The MLC gap was moved under the jaw at an X2 position of 7cm except for the 5x5 field which was placed at an X2 of 5cm; this was to ensure that the dosimetric leaf gap did not affect our measurements. For each field size with and without MLC the average dose for each ROI was taken at depths of 1.5cm (approximate depth of maximum dose for 6MV) and 5cm depth from the surface of the water phantom, SSD (source to surface distance) 100cm.

A typical segment in JTM plans was calculated in Pinnacle for a MLC aperture of 2cm by 1cm located 4cm away from the central axis, while the jaws were set at 12 x 12 cm^2 field size (Figure 2.22). For comparison to the JTM plans, the MLC aperture was collimated to 2mm except for the X1 jaw which was limited to 2cm across central axis (Figure 2.23).
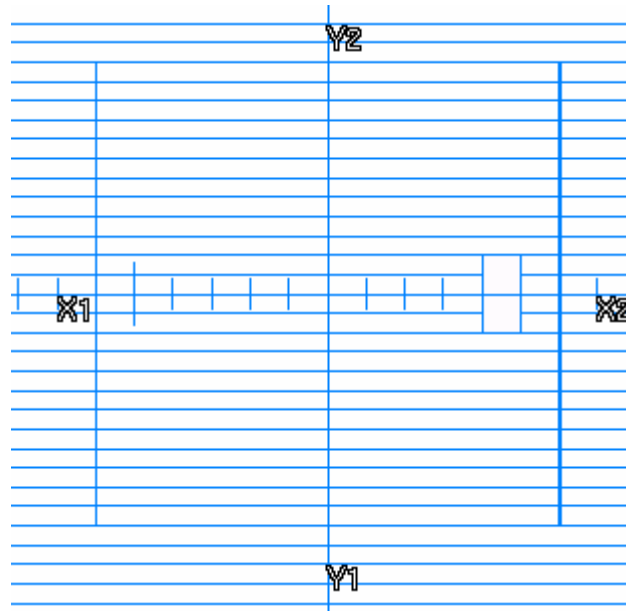
Figure 2.22 Aperture case with jaws out

Average dose to ROIs at 1.5cm and 5cm depths used to find the combination of transmission and scatter in this situation with jaws set to 12 x12 cm^2 field size and an MLC aperture
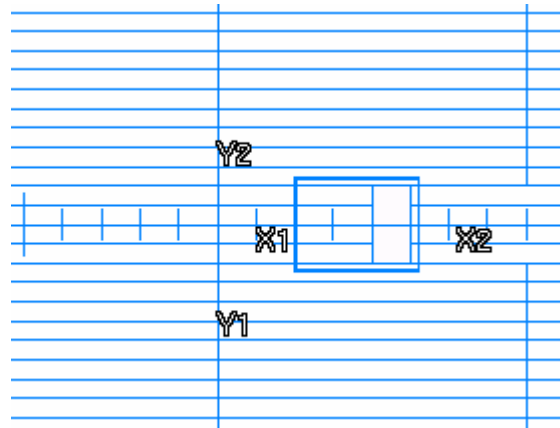
Figure 2.23 Aperture case with jaws in

Average dose to ROIs at 1.5cm and 5cm depths used to find transmission with jaws collimating an MLC aperture to a margin of 2mm to simulate our jaw method; note the X1 jaw is limited to 2cm over central axis and cannot be pulled in to 2mm around the MLC opening.

For all linac measurements, a 0.6cc PTW ion chamber was used in PMMA at depths of approximately 1.5cm and 5cm with SSD 100cm. The collimator remained at 0 degrees and the chamber was positioned towards the gantry so that the active length would average transmission across several leaves. Each situation was measured with enough measurements to ensure no trend in charge accumulated formed.

3 Results

3.1 Treatment Plans

Figures 3.1-3.16 below display each patient's dose-volume-histogram (DVH) and the corresponding Tables 3.1-3.16 show the volumes receiving doses of 5Gy, 10Gy, and 20Gy for the original and JTM plans and the reduction achieved with the JTM plan. The tables displaying head and neck results (Tables 3.11-3.13) also display maximum doses for brainstem and cord and average doses for left and right parotids along with corresponding percent reductions with the JTM plans; this was added as these are parameters looked at when reviewing clinical plans. For thoracic patients the colors in the DVH are as follows: Red = spinal cord, bright green = esophagus, dark blue = Total lung minus GTV, pink = heart, light blue = right lung, dark green = left lung, yellow = liver, light blue = PTV, CTV = yellow, GTV = dark red.
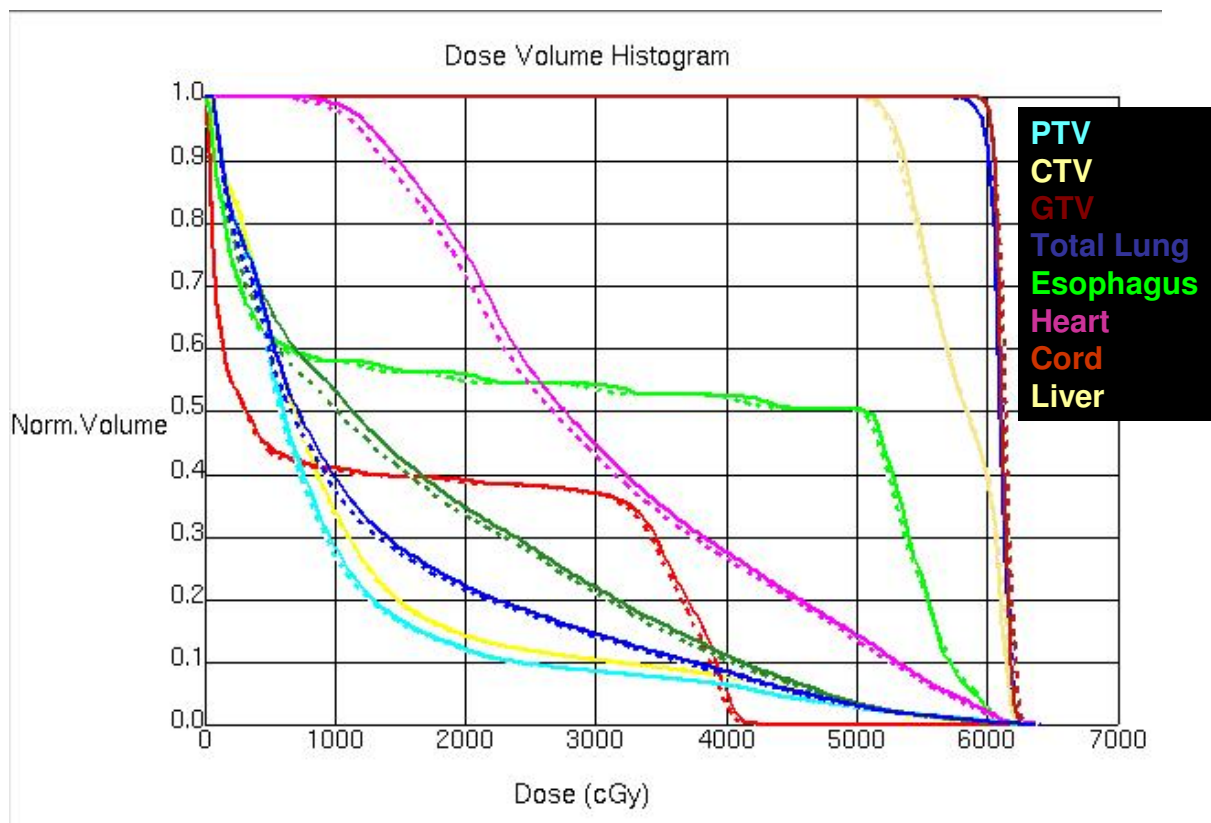
Figure 3.1 Patient Thoracic 1 DVH with JTM plan in dashed lines

		Original	New	%V diff
Total Lung	V5	62.63	59.27	3.36
	V10	39.27	37.30	1.97
	V20	22.03	21.37	0.66
Heart	V5	100.00	100.00	0.00
	V10	98.74	97.91	0.82
	V20	74.99	71.54	3.45
Esophagus	V5	61.98	62.66	-0.68
	V10	57.77	57.77	0.00
	V20	55.64	54.61	1.03
Cord	V5	44.17	43.49	0.68
	V10	40.74	40.48	0.26
	V20	38.80	38.47	0.32
Liver	V5	62.01	61.67	0.33
	V10	33.92	33.48	0.44
	V20	14.14	14.06	0.08

Table 3.1 Patient Thoracic 1 results

Dose Volume Histogram

PTV
CTV
GTV
Total Lung
Esophagus
Heart
Cord
Liver
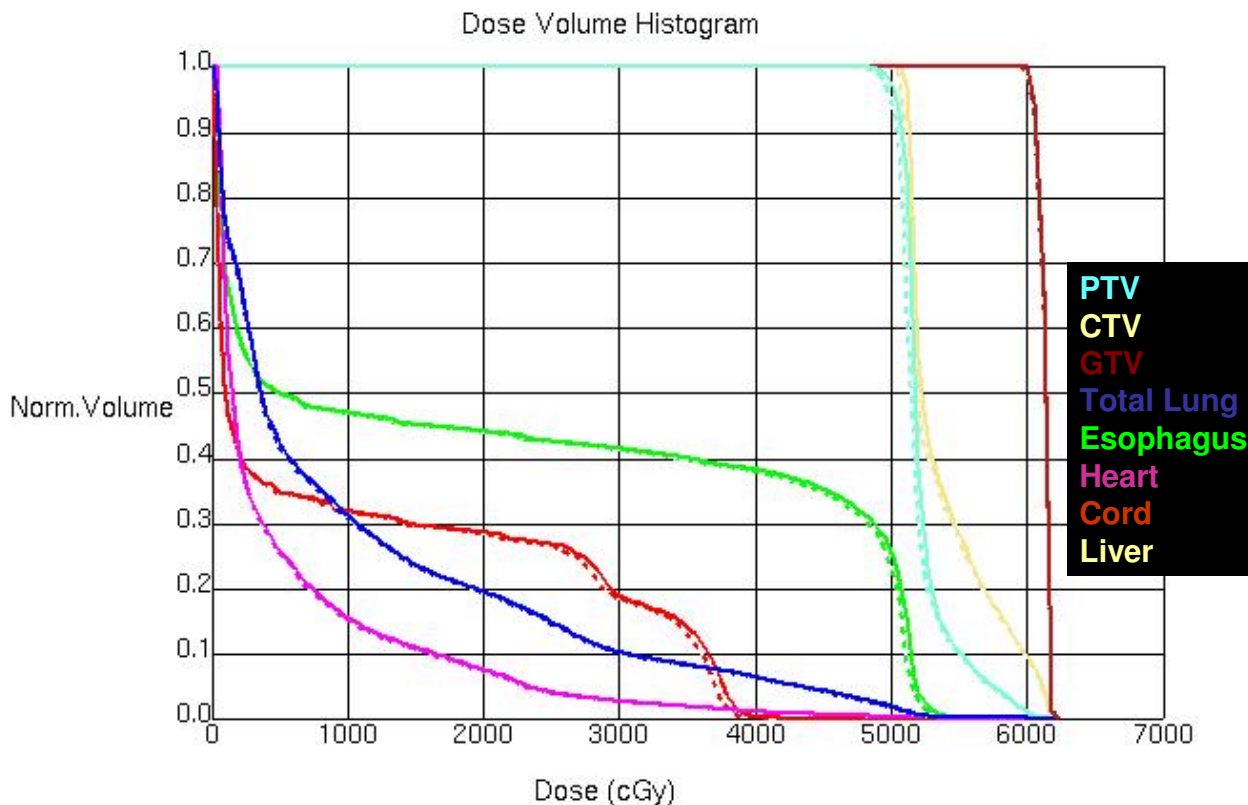
Figure 3.2 Patient Thoracic 2 DVH with JTM plan in dashed lines

		Original	New	%V diff
Total Lung	V5	42.31	41.47	0.84
	V10	31.13	30.68	0.45
	V20	19.43	19.26	0.17
Heart	V5	25.67	25.25	0.42
	V10	15.43	14.98	0.45
	V20	7.42	7.14	0.28
Esophagus	V5	49.87	49.72	0.15
	V10	46.83	46.72	0.11
	V20	43.97	43.81	0.15
Cord	V5	34.59	34.48	0.11
	V10	31.82	31.56	0.26
	V20	28.47	28.29	0.17

Table 3.2 Patient Thoracic 2 results
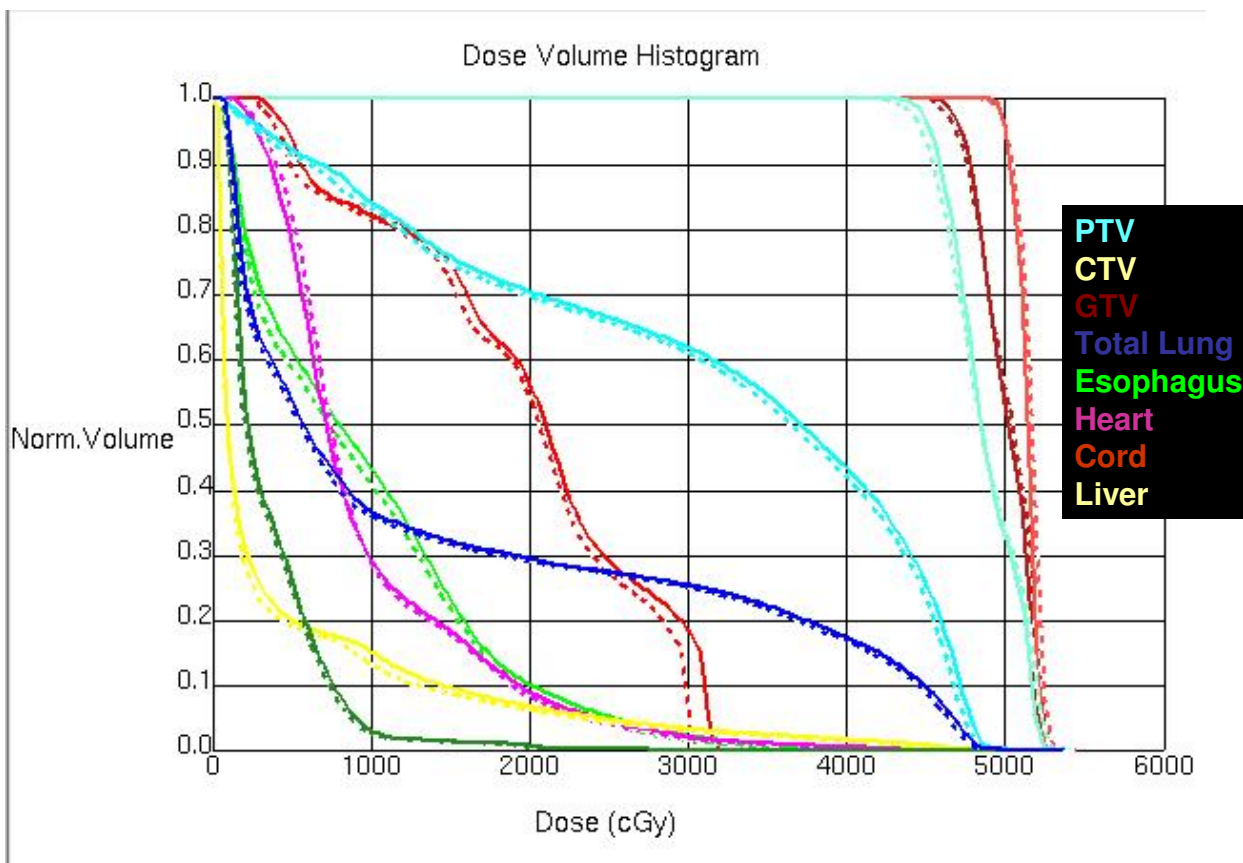
Figure 3.3 Patient Thoracic 3 DVH

		Original	New	%V diff
Total Lung	V5	53.61	52.43	1.18
	V10	36.51	35.76	0.75
	V20	29.30	28.79	0.51
Heart	V5	77.68	81.98	-4.30
	V10	29.03	28.62	0.42
	V20	8.80	8.13	0.67
Esophagus	V5	61.20	58.49	2.71
	V10	43.09	40.69	2.40
	V20	10.03	8.52	1.51
Cord	V5	93.56	89.30	4.26
	V10	81.96	81.37	0.59
	V20	56.39	53.91	2.48
Liver	V5	19.89	19.03	0.86
	V10	15.06	13.11	1.95
	V20	6.61	6.04	0.57

Table 3.3 Patient Thoracic 3 results
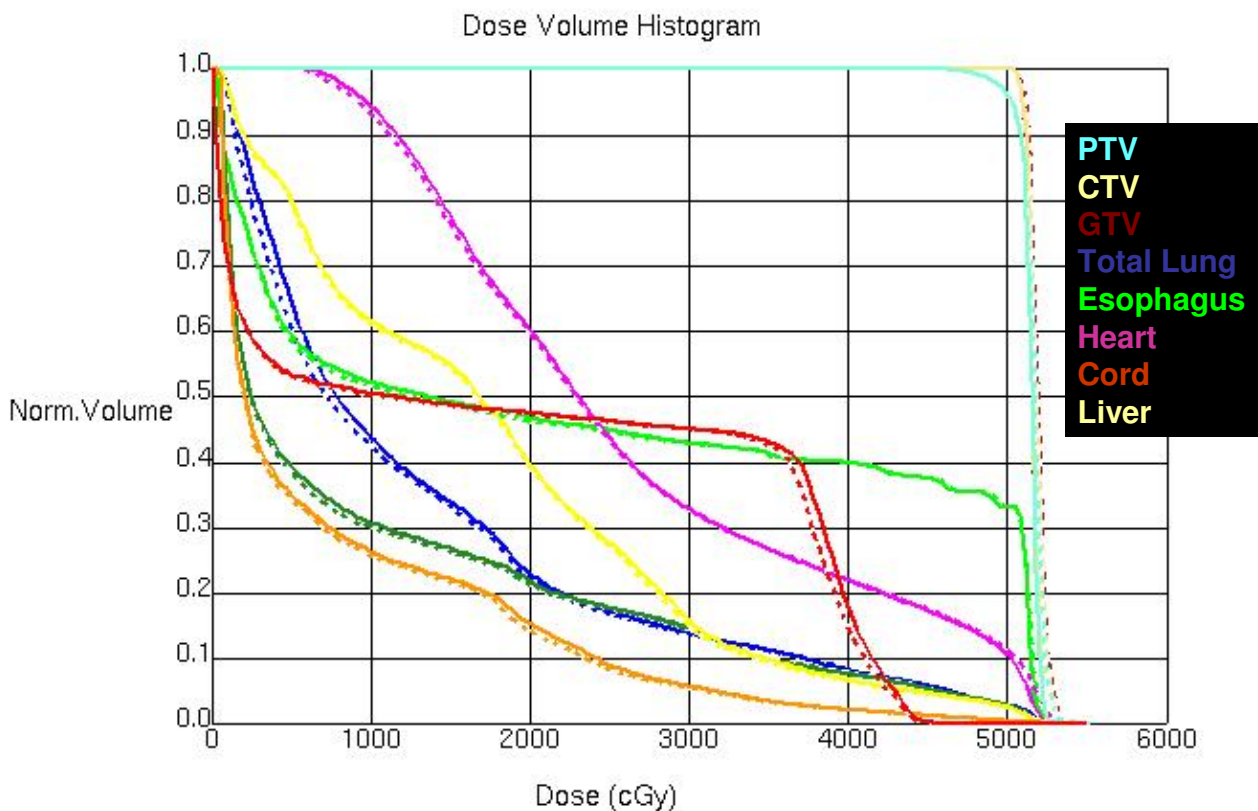
Figure 3.4 Patient Thoracic 4 DVH

		Original	New	%V diff
Total Lung	V5	64.35	60.25	4.10
	V10	43.69	42.30	1.39
	V20	22.75	22.05	0.70
Heart	V5	100.00	100.00	0.00
	V10	94.14	92.89	1.25
	V20	60.08	59.52	0.55
Esophagus	V5	59.22	58.37	0.85
	V10	51.97	51.46	0.51
	V20	46.56	45.95	0.61
Cord	V5	53.07	52.79	0.28
	V10	50.19	49.89	0.30
	V20	47.28	47.15	0.13
Liver	V5	79.91	79.48	0.43
	V10	61.43	60.96	0.47
	V20	39.51	39.09	0.43

Table 3.4 Patient Thoracic 4 results
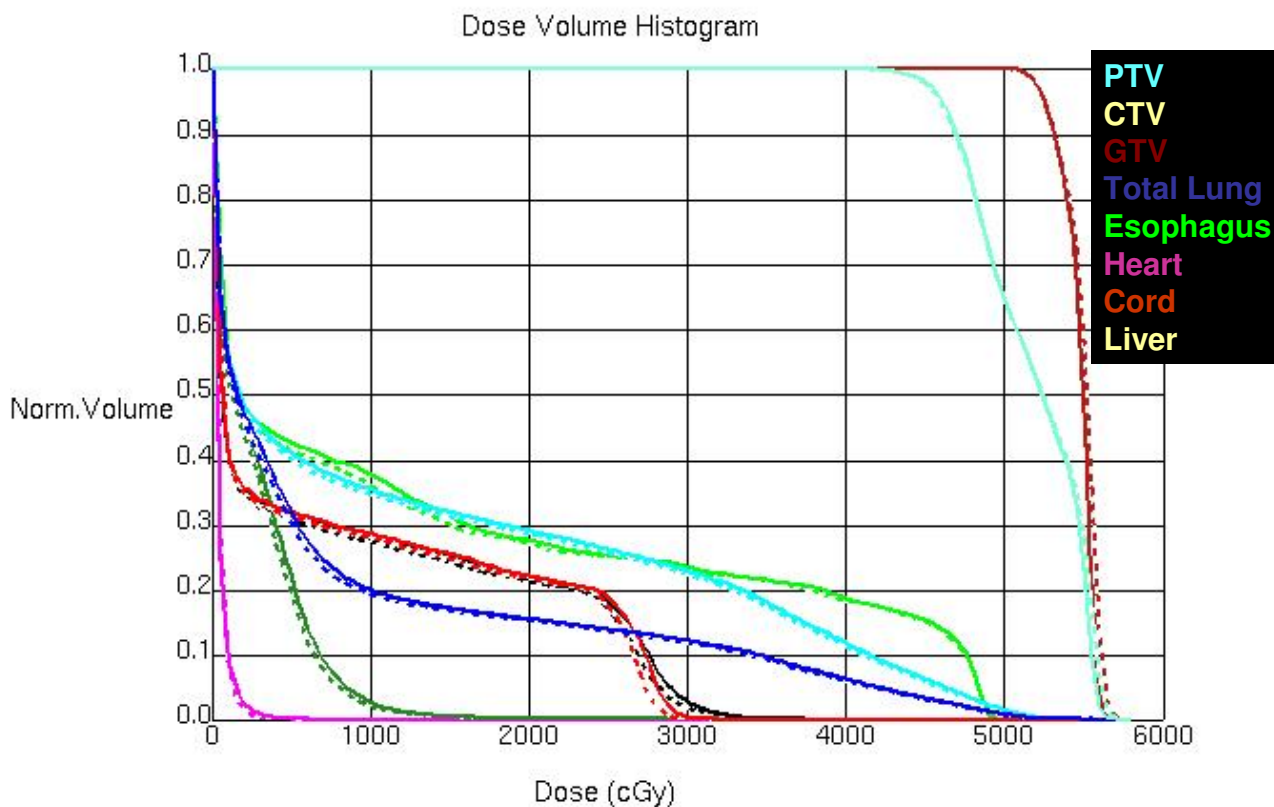
Figure 3.5 Patient Thoracic 5 DVH

		Original	New	%V diff
Total Lung	V5	31.86	30.18	1.68
	V10	19.93	19.24	0.69
	V20	15.38	15.12	0.26
Heart	V5	0.05	0.01	0.05
	V10	0.00	0.00	0.00
	V20	0.00	0.00	0.00
Esophagus	V5	42.49	41.37	1.12
	V10	37.56	35.87	1.68
	V20	27.58	26.98	0.60
Cord	V5	31.91	31.02	0.89
	V10	28.45	27.90	0.55
	V20	22.00	21.66	0.34

Table 3.5 Patient Thoracic 5 results
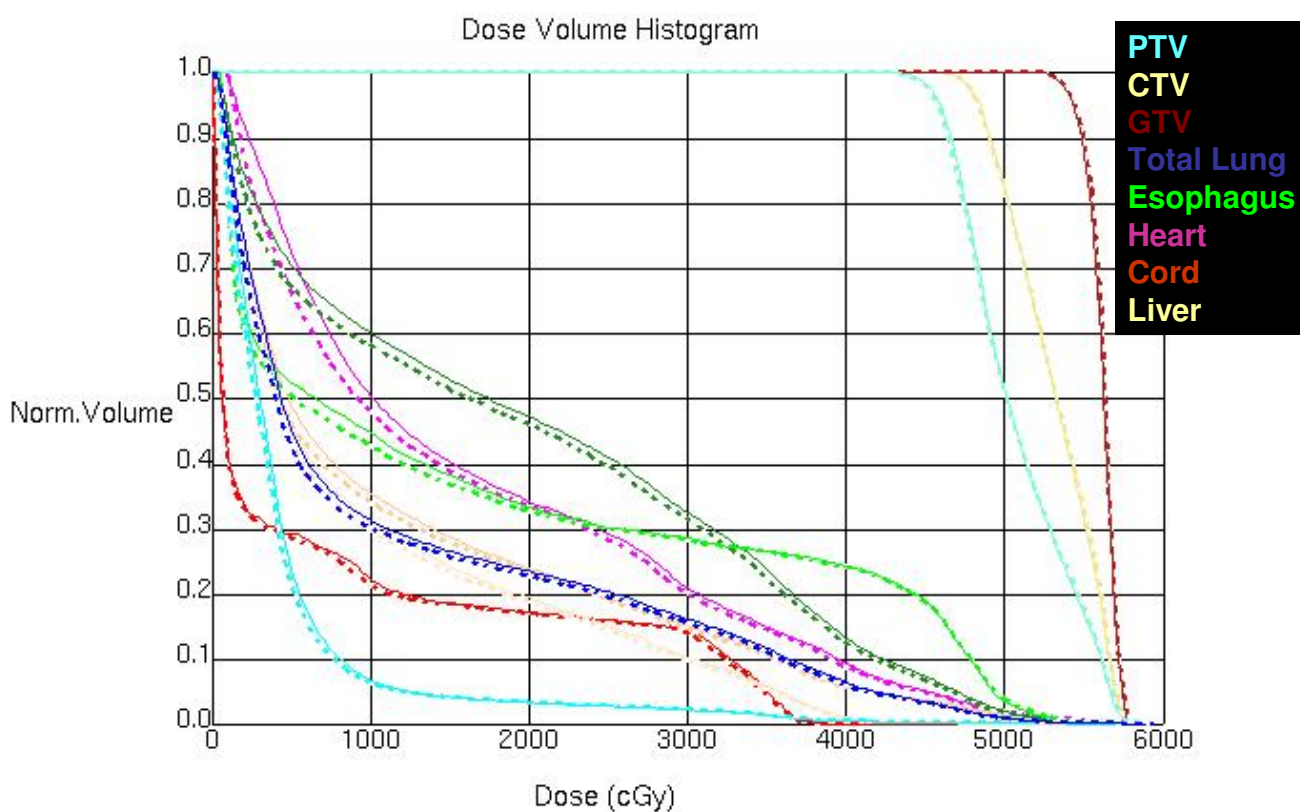
Figure 3.6 Patient Thoracic 6 DVH

		Original	New	%V diff
Total Lung	V5	45.32	42.41	2.91
	V10	31.20	30.10	1.11
	V20	23.35	22.79	0.56
Heart	V5	72.57	66.31	6.26
	V10	50.33	47.71	2.62
	V20	34.05	33.31	0.74
Esophagus	V5	52.13	50.32	1.81
	V10	44.53	42.65	1.89
	V20	33.16	32.57	0.59
Cord	V5	29.11	28.53	0.58
	V10	22.15	21.18	0.97
	V20	17.04	16.90	0.14

Table 3.6 Patient Thoracic 6 results
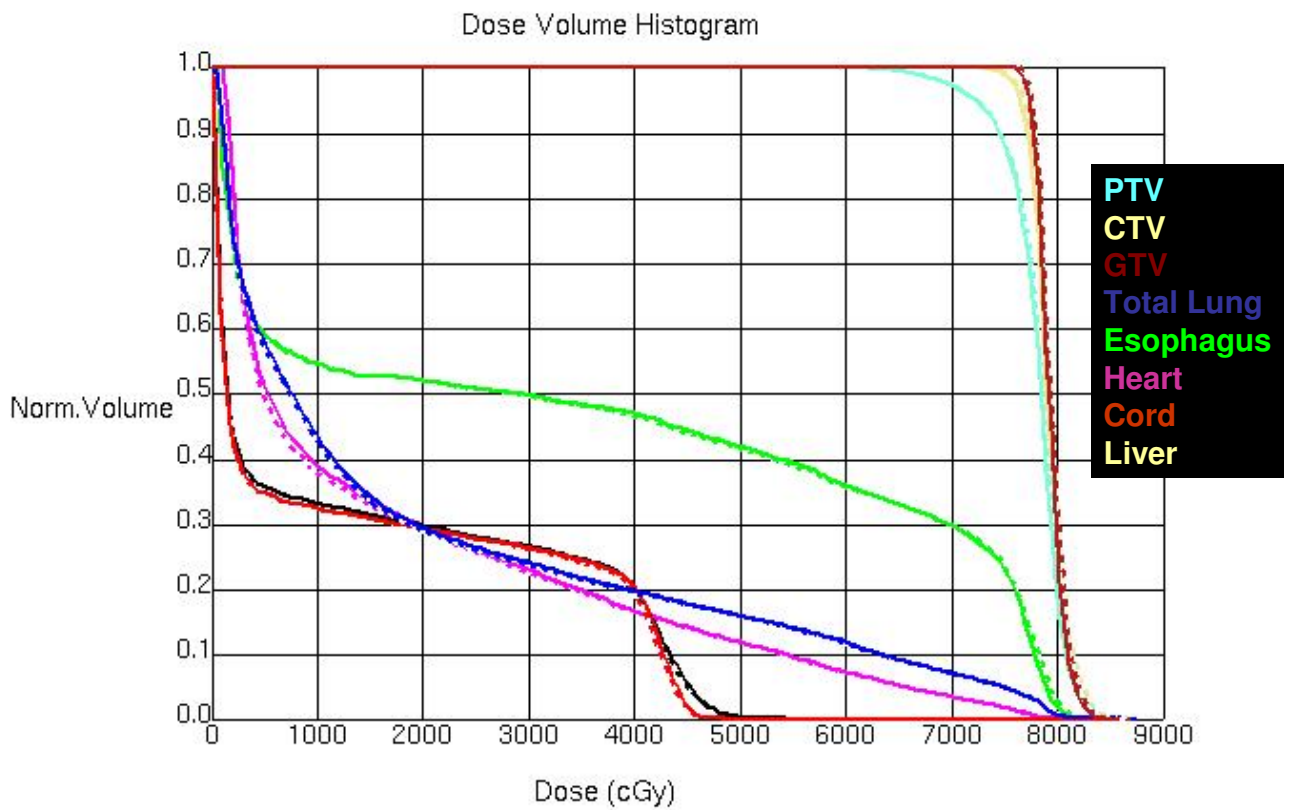
Figure 3.7 Patient Thoracic 7 DVH

		Original	New	%V diff
Total Lung	V5	56.95	56.01	0.94
	V10	42.66	41.92	0.74
	V20	28.89	28.43	0.46
Heart	V5	51.12	49.33	1.79
	V10	38.68	37.68	1.00
	V20	29.54	28.96	0.58
Esophagus	V5	59.14	58.72	0.42
	V10	54.44	54.39	0.05
	V20	51.83	51.83	0.00
Cord	V5	34.53	34.54	-0.01
	V10	32.13	32.11	0.02
	V20	29.07	29.04	0.02

Table 3.7 Patient Thoracic 7 results
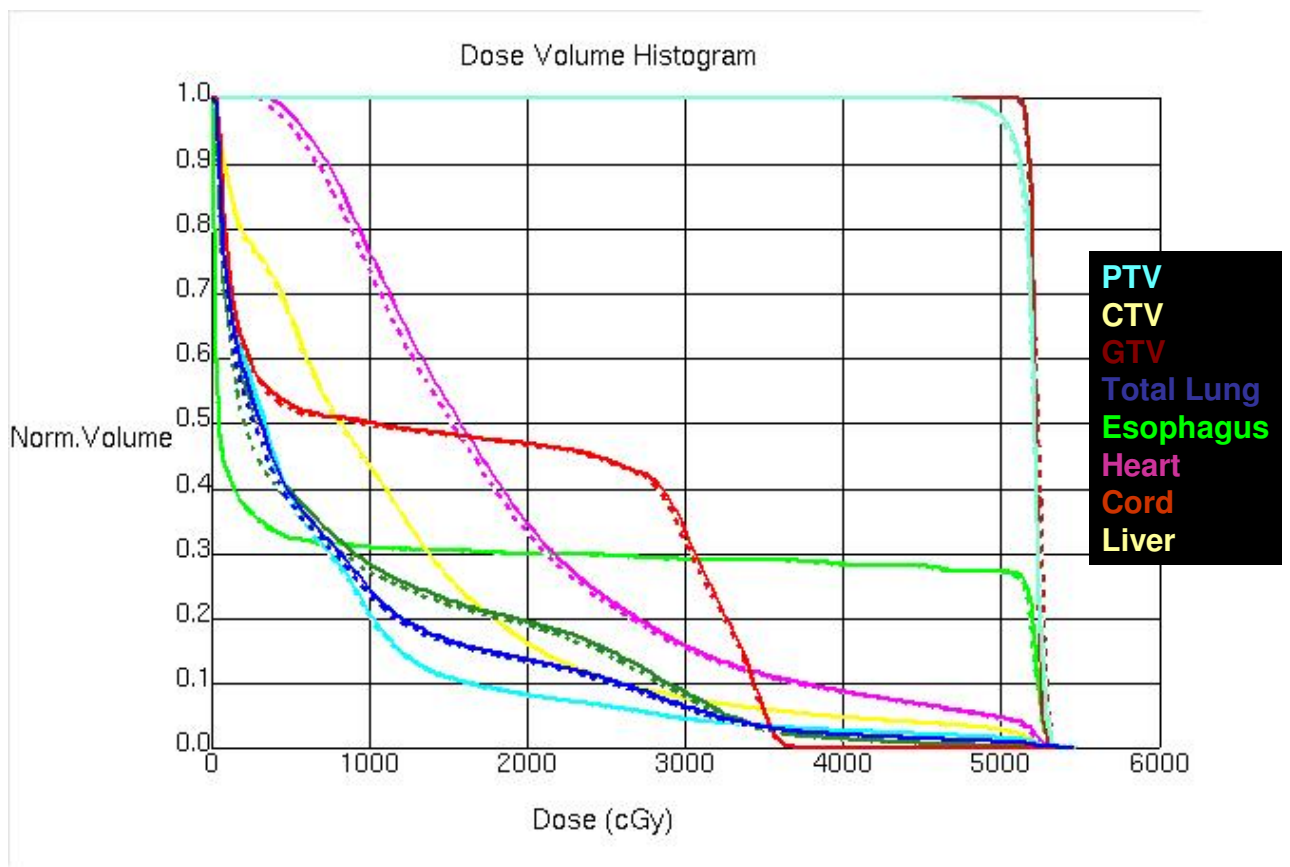
Figure 3.8 Patient Thoracic 8 DVH

43

		Original	New	%V diff
Total Lung	V5	39.04	37.72	1.33
	V10	24.41	23.52	0.89
	V20	13.47	13.13	0.34
Heart	V5	97.47	95.66	1.81
	V10	76.49	73.61	2.88
	V20	34.49	32.97	1.52
Esophagus	V5	32.13	32.09	0.04
	V10	30.72	30.68	0.04
	V20	29.70	29.68	0.02
Cord	V5	52.84	52.04	0.80
	V10	49.95	49.61	0.34
	V20	46.67	46.46	0.21
Liver	V5	66.69	65.82	0.87
	V10	43.61	43.39	0.22
	V20	16.14	16.01	0.13

Table 3.8 Patient Thoracic 8 results
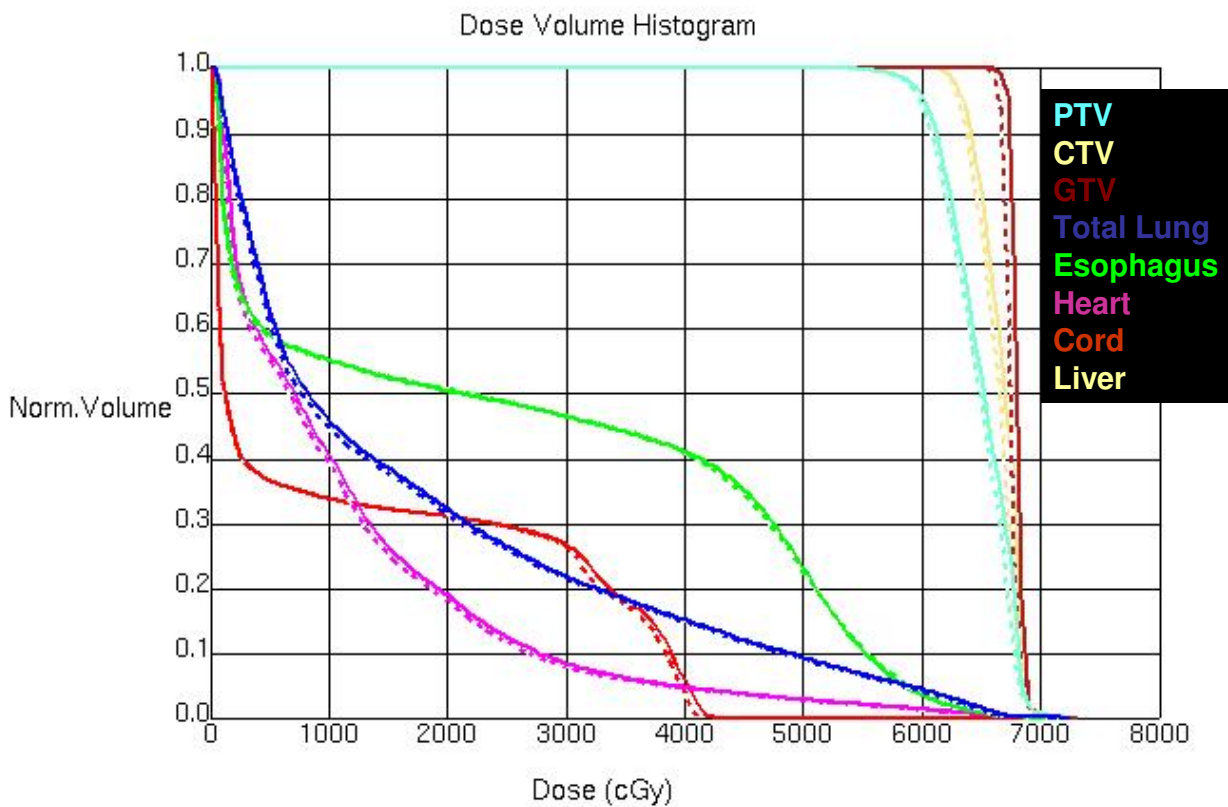
Figure 3.9 Patient Thoracic 9 DVH

		Original	New	%V diff
Total Lung	V5	62.73	60.83	1.90
	V10	45.76	44.54	1.22
	V20	32.09	31.25	0.84
Heart	V5	56.06	54.97	1.09
	V10	40.45	39.21	1.25
	V20	18.81	17.98	0.83
Esophagus	V5	58.94	58.61	0.34
	V10	55.01	54.99	0.02
	V20	50.15	50.44	-0.30
Cord	V5	36.53	36.50	0.03
	V10	33.61	33.61	0.00
	V20	30.92	30.92	0.00

Table 3.9 Patient Thoracic 9 results
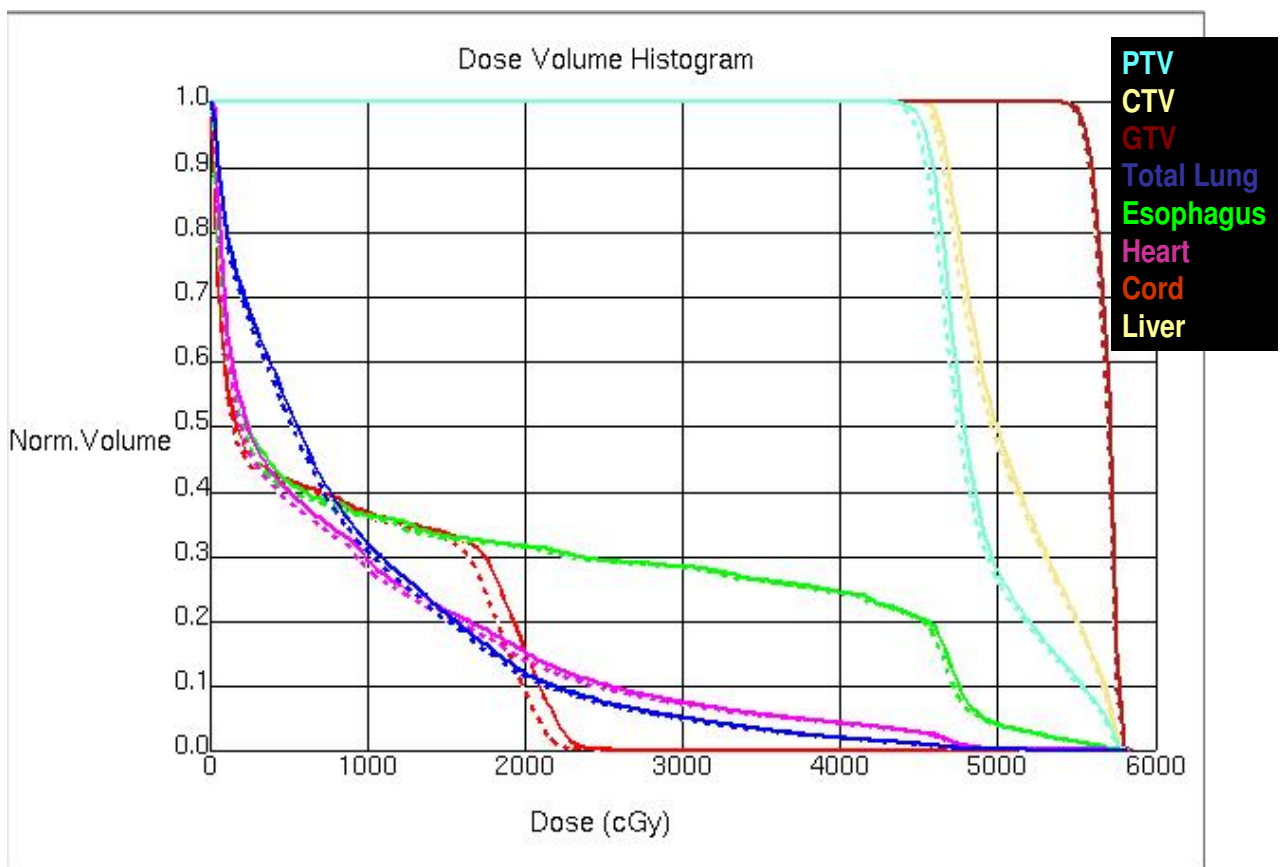
Figure 3.10 Patient Thoracic 10 DVH

45

		Original	New	%V diff
Total Lung	V5	53.00	51.19	1.81
	V10	31.90	30.70	1.20
	V20	11.89	11.34	0.55
Heart	V5	39.90	38.34	1.56
	V10	29.34	27.89	1.45
	V20	15.09	13.93	1.16
Esophagus	V5	41.39	40.10	1.28
	V10	36.17	35.82	0.34
	V20	31.37	31.20	0.17
Cord	V5	41.66	40.99	0.68
	V10	36.61	35.92	0.69
	V20	15.30	8.97	6.33

Table 3.10 Patient Thoracic 10 results
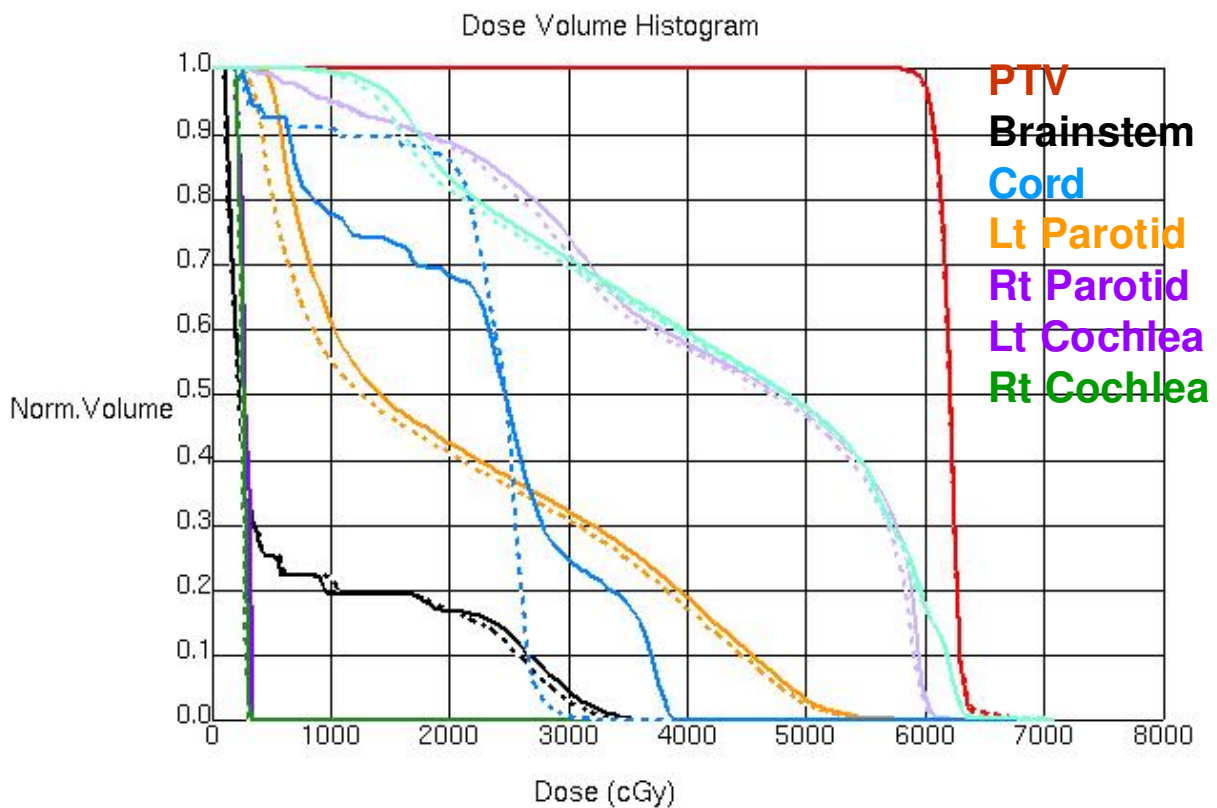
Figure 3.11 Patient Head and Neck 1 DVH

For this patient the colors in the DVH are as follows: brainstem = black, right parotid = lavender, left parotid = orange, spinal cord = blue, right cochlea = dark green, left cochlea = purple, and the target = red

		Original	New	%Diff
Brainstem	**V5**	25.11	25.1	0
	V10	19.11	21.8	-2.66
	V20	16.56	16.6	-0.07
(cGy)	**Max**	3523.00	3431	2.61
Rt parotid	**V5**	98.94	98.9	0.07
	V10	94.93	94.6	0.28
	V20	88.38	88	0.40
(cGy)	**Average**	4243.50	4174	1.65
Lt parotid	**V5**	96.99	80.3	16.69
	V10	61.00	55.1	5.94
	V20	42.41	40.8	1.62
(cGy)	**Average**	2117.70	1975	6.74
Cord	**V5**	92.26	92.3	0.00
	V10	77.36	90.6	-13.24
	V20	68.14	85.7	-17.55
(cGy)	**Max**	3876.00	3180	17.96

Table 3.11 Patient Head and Neck 1 results

Figure 3.12 Patient Head and Neck 2 DVH

For this patient the colors in the DVH are as follows: brainstem = orange, spinal cord = brown, left parotid = light blue, right parotid = pink, right cochlea = dark green, left cochlea = purple, and the target = red.

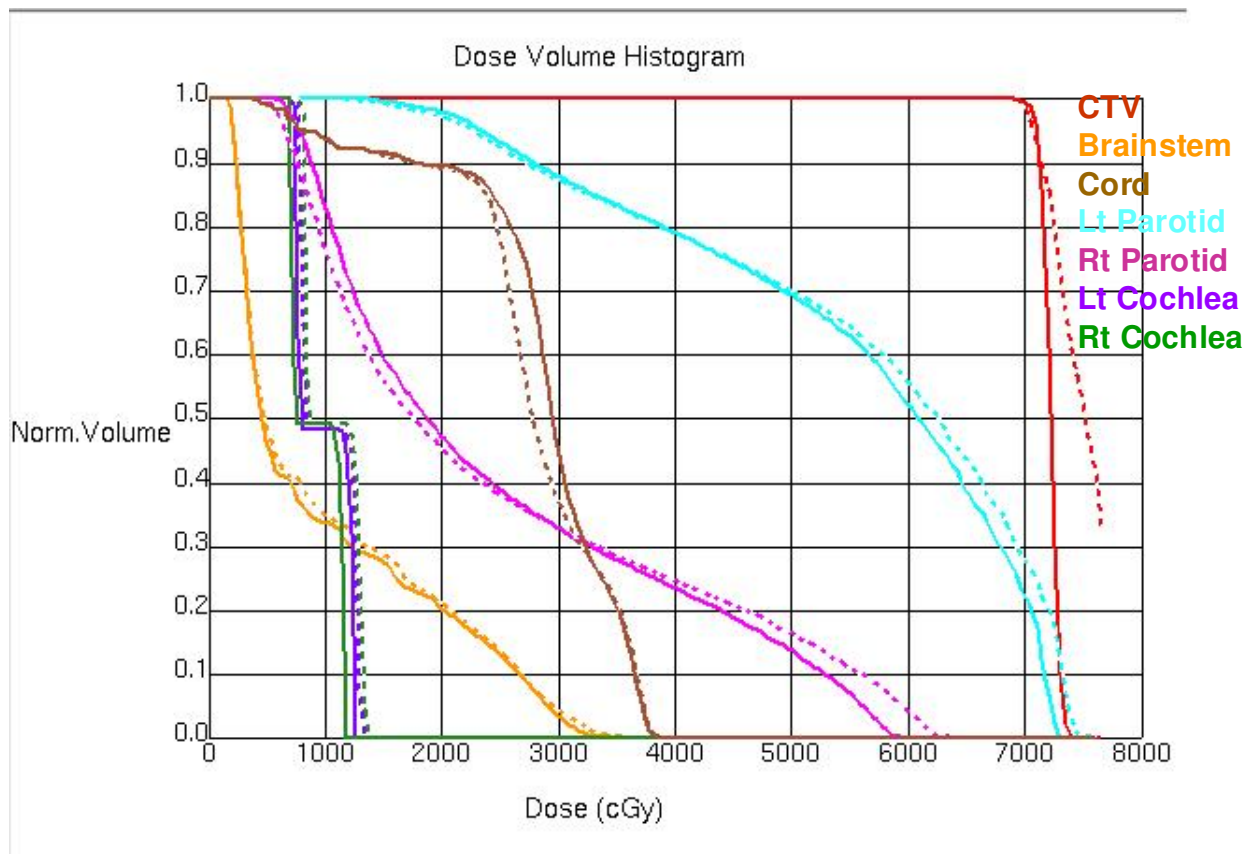|		Original	New	%Diff
Brainstem	V5	46.05	48.70	-2.65
	V10	33.55	34.71	-1.17
	V20	20.03	20.88	-0.85
(cGy)	Max	3390	3540	-4.42
Rt parotid	V5	100.00	99.69	0.31
	V10	82.90	76.31	6.59
	V20	47.14	45.02	2.12
(cGy)	Average	2506.1	2508.2	-0.08
Lt parotid	V5	100.00	100.00	0.00
	V10	100.00	100.00	0.00
	V20	97.76	97.04	0.72
(cGy)	Average	5532.9	5622.1	-1.61
Cord	V5	100.00	99.11	0.89
	V10	99.11	93.67	5.44
	V20	89.22	88.88	0.35
(cGy)	Max	3830	3850	-0.52

Table 3.12 Patient Head and Neck 2 results
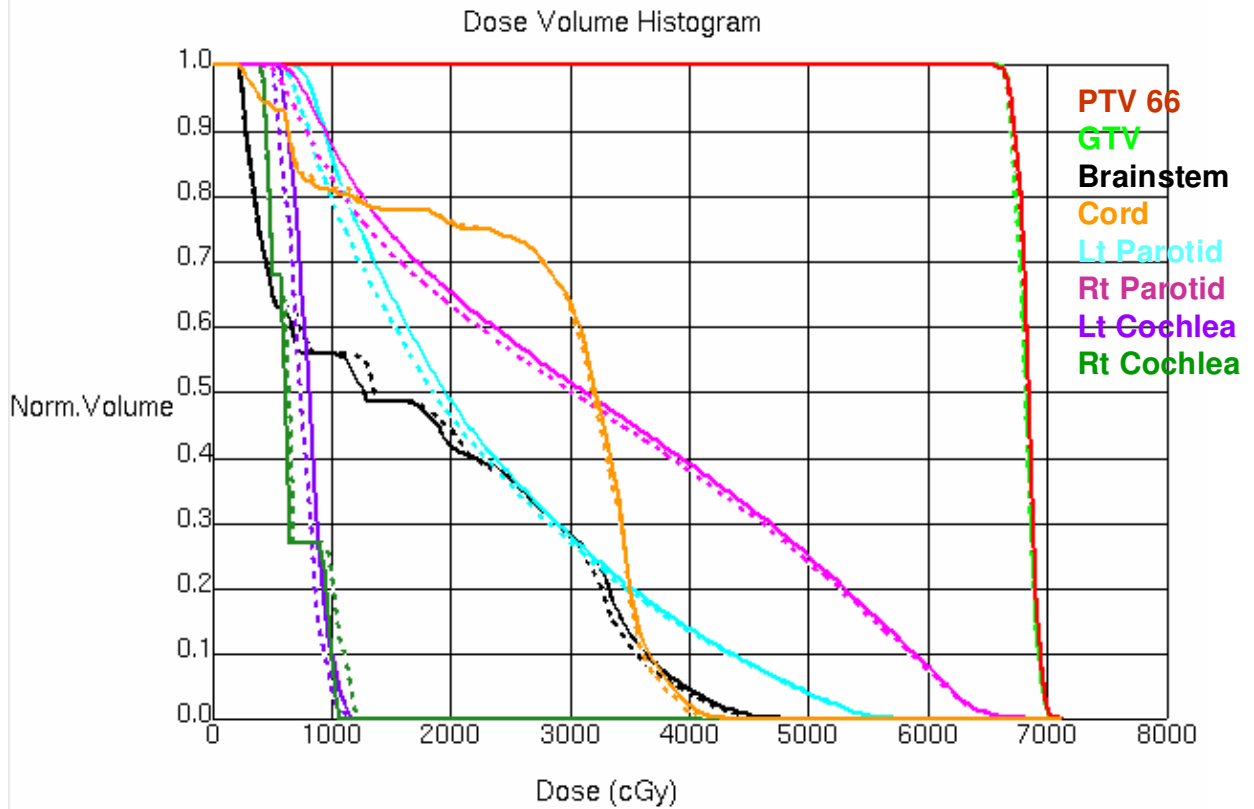
Figure 3.13 Patient Head and Neck 3 DVH

For this patient the colors in the DVH are as follows: right parotid = pink, left parotid = light

blue, spinal cord = orange, brainstem = black, right cochlea = dark green, left cochlea =

purple, and the target = red.

		Original	New	%Diff
Brainstem	**V5**	**64.61**	**64.88**	**-0.27**
	V10	**55.74**	**55.74**	**0.00**
	V20	**41.47**	**44.03**	**-2.56**
(cGy)	**Max**	**4718**	**4657**	**1.29**
Rt parotid	**V5**	**100.00**	**99.26**	**0.74**
	V10	**87.76**	**82.74**	**5.02**
	V20	**65.05**	**63.07**	**1.98**
(cGy)	**Average**	**3260.6**	**3160.7**	**3.06**
Lt parotid	**V5**	**100.00**	**100.00**	**0.00**
	V10	**86.05**	**79.37**	**6.68**
	V20	**48.48**	**46.01**	**2.47**
(cGy)	**Average**	**2310**	**2219.4**	**3.92**
Cord	**V5**	**93.60**	**93.66**	**-0.06**
	V10	**80.74**	**80.97**	**-0.23**
	V20	**75.60**	**76.00**	**-0.40**
(cGy)	**Max**	**4266**	**4212**	**1.27**

Table 3.13 Patient Head and Neck 3 results
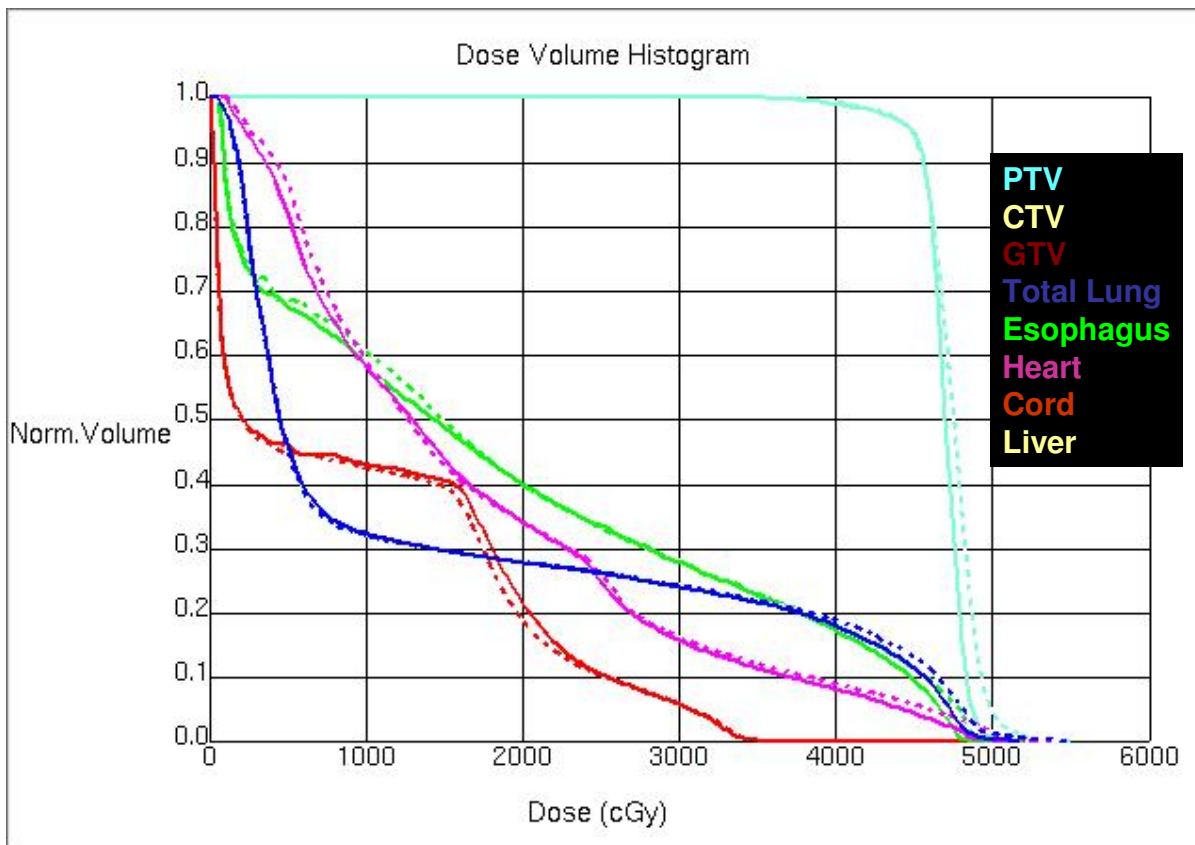
Figure 3.14 Patient Pediatric 1 DVH

For this patient the colors in the DVH are as follows: spinal cord = red, total lung minus

GTV = blue, esophagus = green, heart = pink, and the target = light blue.

		Original	New	%V diff
Total Lung	V5	45.73	45.05	0.69
	V10	32.15	31.84	0.31
	V20	25.30	27.61	-2.32
Heart	V5	81.69	86.44	-4.76
	V10	58.01	59.07	-1.06
	V20	33.99	33.97	0.02
Esophagus	V5	67.24	68.29	-1.05
	V10	58.53	60.43	-1.90
	V20	39.72	39.69	0.03
Cord	V5	45.77	44.63	1.14
	V10	42.80	42.24	0.56
	V20	21.43	18.61	2.82

Table 3.14 Patient Pediatric 1 results

Dose Volume Histogram

Legend:
- PTV
- CTV
- GTV
- Total Lung
- Esophagus
- Heart
- Cord
- Liver

Figure 3.15 Patient Pediatric 2 DVH

For this patient the colors in the DVH are as follows: liver minus GTV = yellow, heart = pink, esophagus = green, spinal cord = red, total lung = blue, and the target = light blue.

		Original	New	%V diff
Total Lung	V5	45.35	42.35	3.00
	V10	32.30	31.52	0.78
	V20	23.73	23.29	0.45
Heart	V5	91.91	86.72	5.19
	V10	71.05	69.19	1.86
	V20	32.81	31.94	0.86
Esophagus	V5	50.48	50.18	0.30
	V10	43.03	40.00	3.03
	V20	25.09	23.76	1.33
Cord	V5	63.75	61.29	2.45
	V10	49.06	47.63	1.43
	V20	21.89	21.52	0.37
Liver	V5	74.91	73.83	1.08
	V10	67.52	66.29	1.24
	V20	52.63	51.69	0.94

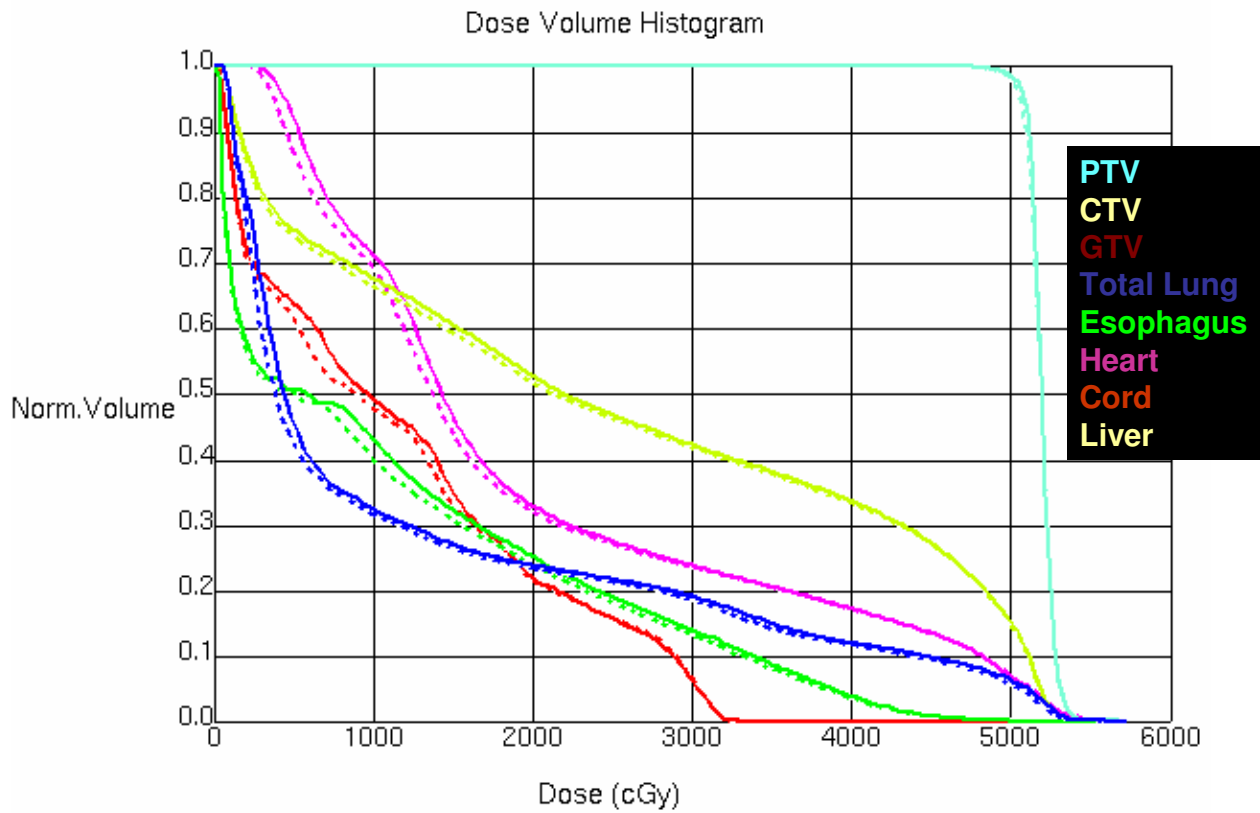**Table 3.15 Patient Pediatric 2 results**

Dose Volume Histogram
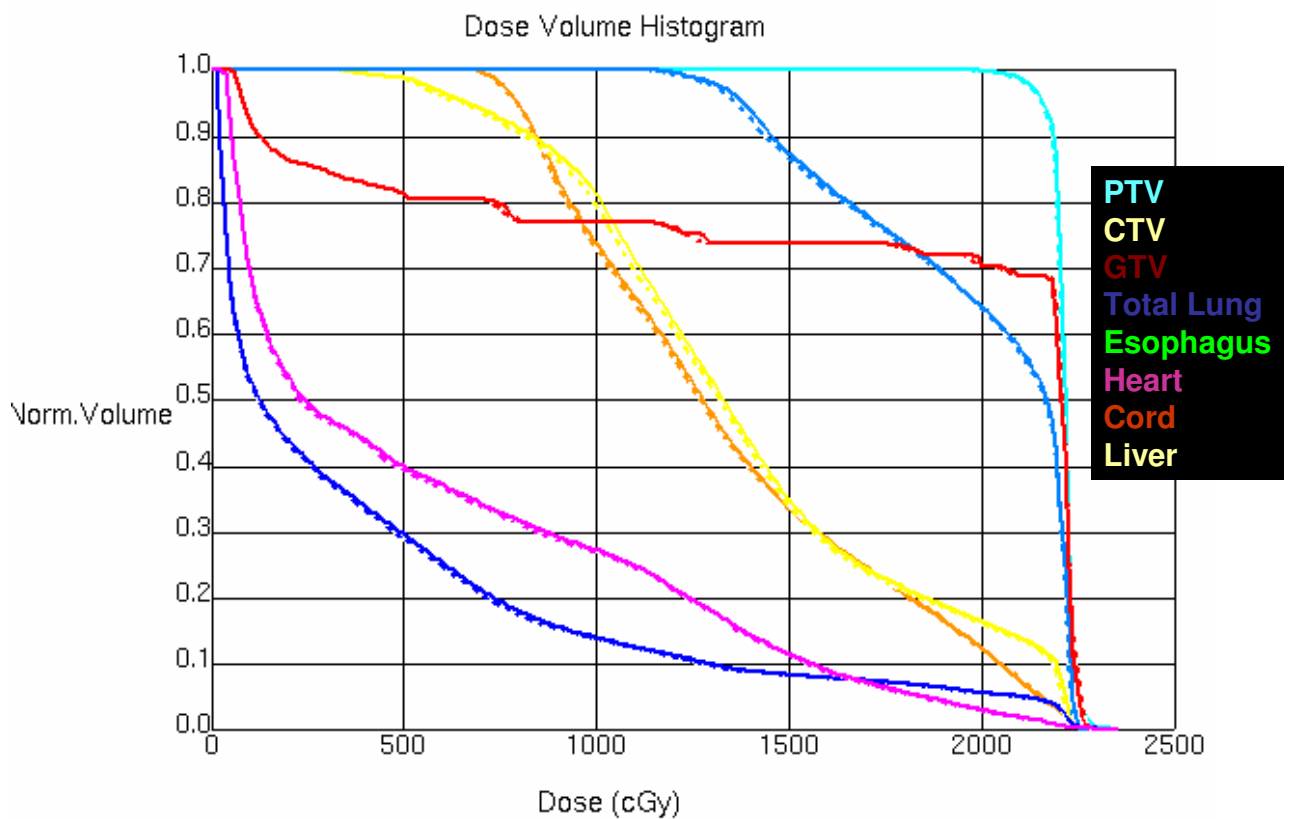
Figure 3.16 Patient Pediatric 3 DVH

For this patient the colors in the DVH are as follows: spinal cord = red, total lung = dark

blue, heart = pink, liver = yellow, left kidney = orange, right kidney = blue and the target =

light blue.

		Original	New	%V diff
Total Lung	V5	29.47	28.79	0.68
	V10	13.79	13.60	0.19
	V20	5.45	5.36	0.09
Heart	V5	39.69	39.15	0.54
	V10	27.06	26.75	0.30
	V20	2.89	2.72	0.17
Liver	V5	98.60	98.53	0.07
	V10	80.99	79.18	1.81
	V20	16.37	16.08	0.29
Lt Kidney	V5	100.00	100.00	0.00
	V10	79.35	78.46	0.89
	V20	13.15	13.10	0.06
Rt Kidney	V5	100.00	100.00	0.00
	V10	100.00	100.00	0.00
	V20	64.07	63.67	0.40

Table 3.16 Patient Pediatric 3 results

Below is Table 3.17 which lists each patient and their respective integral dose reduction

with the JTM plan compared to the original plan. The first column shows the integral dose

difference using the structure external in Equation 1.1 which encompasses all other contours.

The second column shows the integral dose difference using the structure external minus

target in Equation 1.1. Figure 3.17 shows an axial view of the isodose distribution for

original and JTM plans for patient T 10. One limitation of this jaw method is the physical

limitation of the X jaws to only over travel the central axis by 2cm and the Y jaws to only

over travel the central axis by 10cm. A number of segments did not have an X jaw

collimating one side of the MLC aperture to 2mm because of this limitation; Table 3.18

attempts to quantify how this limitation affected each patient.

% Difference Integral Dose											
T 1	1.86	2.39	**T 5**	3.25	3.99	**T 9**	1.84	2.07	**HN 3**	1.74	1.94
T 2	1.73	1.96	**T 6**	3.82	4.37	**T 10**	2.99	3.33	**Ped 1**	-0.18	0.46
T 3	1.88	2.63	**T 7**	1.08	1.47	**HN 1**	1.33	1.7	**Ped 2**	1.53	2.65
T 4	1.39	1.74	**T 8**	1.85	2.16	**HN 2**	-1.09	-1.03	**Ped 3**	0.70	1.00

Table 3.17 Integral Dose Differences

Each patient's integral dose reduction from the original plan; values given are percent

differences between the original and JTM plan's integral dose. First column uses external

structure, second column uses external minus target structure.
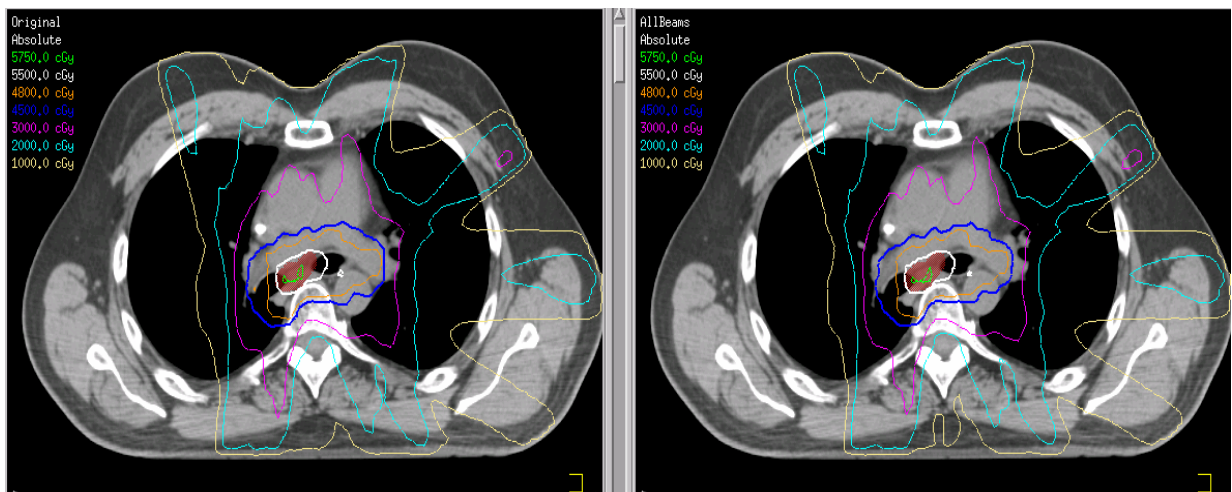
% Beams Jaw Limited of the Total JTM Beams							
T 1	14.0	**T 5**	16.0	**T 9**	3.2	**HN 3**	23.3
T 2	14.5	**T 6**	16.2	**T 10**	4.8	**Ped 1**	21.4
T 3	16.3	**T 7**	12.4	**HN 1**	21.4	**Ped 2**	19.8
T 4	10.6	**T 8**	1.2	**HN 2**	18.3	**Ped 3**	15.2

Table 3.18 Percentage of beams in each patient's JTM plan that experience a jaw limitation and therefore cannot completely collimated the MLC aperture to a margin of 2mm

As some target DVHs show either the original or JTM plan with a higher dose going to a smaller volume, maximum dose was evaluated between the two plans. Table 3.19 lists all patients and their respective percent difference in maximum dose in going from the original plan to the JTM plan. All original and JTM plan maximum doses were located within the target.

% Difference in Max Dose							
T 1	-0.38	**T 5**	-0.47	**T 9**	0.44	**HN 3**	0.29
T 2	-0.18	**T 6**	-0.65	**T 10**	-0.12	**Ped 1**	-5.63
T 3	-0.97	**T 7**	-2.39	**HN 1**	-3.07	**Ped 2**	1.74

T 4	-1.61	T 8	-0.66	HN 2	-6.88	Ped 3	-0.77

Table 3.19 Percent difference between original and JTM plan maximum doses

3.2 Off-axis output factors

We determined off-axis output factors using Pinnacle (Figure 3.18). We found that the output factors decrease as the field is moved further from the central axis, and that this effect was larger for larger field sizes.
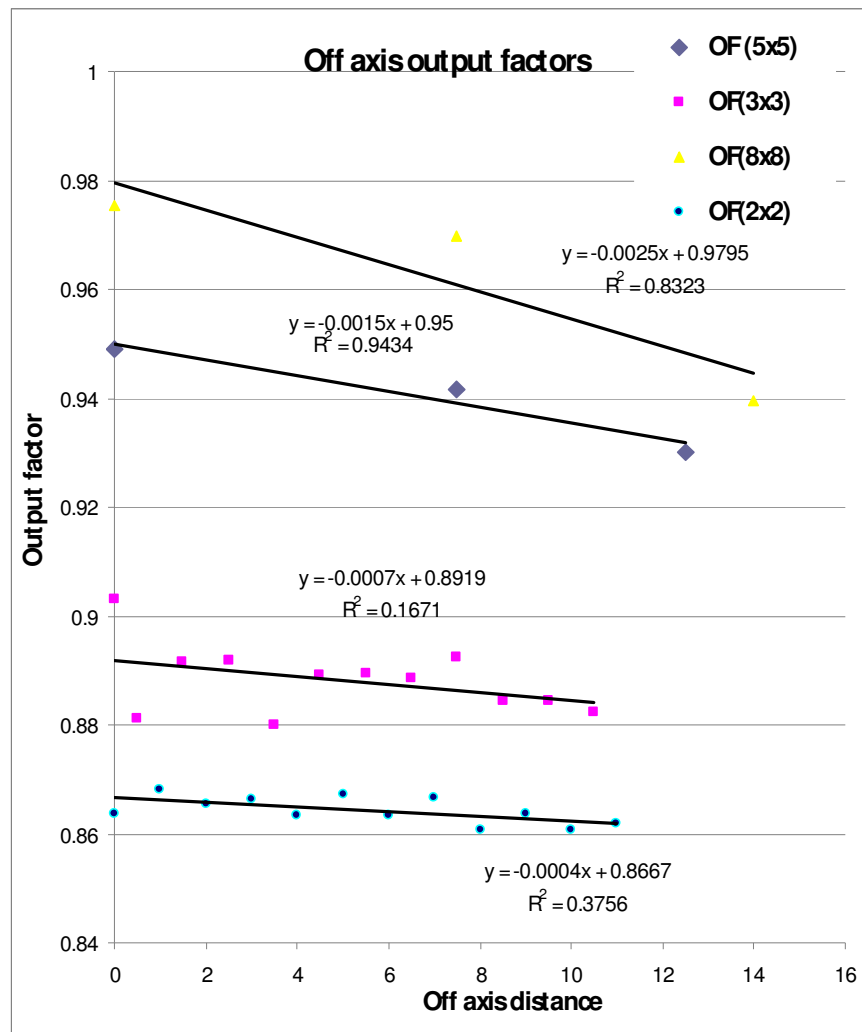
Figure 3.18 Calculated off axis output factors for various field sizes

3.3 Measurements

Table 3.20 shows the transmission measurement results for a depth of 1.5cm comparing percent transmitted for each field combination for Pinnacle and our actual measurements. Table 3.21 shows the same but at a depth of 5cm. The Aperture jaws out refers to Figure 2.22 and the Aperture jaws in refers to Figure 2.23 in the Methods section; both are normalized to open. The absolute difference is taken as the percent measured transmission minus the percent calculated transmission.

Transmission	Measured (%)	Pinnacle (%)	Absolute Difference
5x5	1.48	1.68	-0.20
10x10	1.53	1.60	-0.07
12x12	1.57	1.59	-0.02
Aperture jaws out	1.69	1.62	0.07
Aperture jaws in	0.08	0.03	0.05

Table 3.20 Transmission measurements and Pinnacle Calculations

Measured and Pinnacle estimate of transmission at 1.5cm depth for fields with MLC and jaws at 12x12, 10x10 and 5x5; transmission also for the aperture case with jaws at 12x12 normalized to open field and the aperture case with jaws pulled in normalized to open field and finally the aperture case with jaws in normalized to jaws out at 12x12. The absolute

difference is taken as the percent measured transmission minus the percent calculated transmission.

Transmission	Measured (%)	Pinnacle (%)	Absolute Difference
5x5	1.51	1.68	-0.17
10x10	1.55	1.60	-0.05
12x12	1.59	1.59	0
Aperture jaws out	1.72	1.66	0.06
Aperture jaws in	0.14	0.07	0.08

Table 3.21 Transmission measurements and Pinnacle Calculations

Measured and Pinnacle estimate of transmission at 5cm depth for fields with MLC and jaws at 12x12, 10x10 and 5x5; transmission for the aperture case with jaws at 12x12 normalized to open field and the aperture case with jaws pulled in normalized to open field and finally the aperture case with jaws in normalized to jaws out at 12x12. The absolute difference is taken as the percent measured transmission minus the percent calculated transmission.

4 Discussion

The results in section 3.1 demonstrate an overall reduction in normal tissue dose for the JTM plans compared to the original plans, albeit a small reduction for most tissues. Most patients had less than a 2% improvement in V5, V10 and V20 for their normal tissues. The greatest improvement of lung V5 and V20 were 4.10% and 0.84% respectively. The most volume reduction pertaining to 5, 10 or 20Gy for a normal tissue structure across all patients was 16.69% of a left parotid and the least improvement was -17.55% of the spinal cord; both maximum and minimum improvements occurred for head and neck patient 1. Generally for all structures and patients V5 showed the largest improvement and V20 the least improvement. There was no uniform shift in DVH curves indicating improvement across a single structure was well varied for V5, V10 and V20, and no uniform shift across all normal tissue structure DVH curves for a single patient indicating a patient may experience more sparing for one structure over another. Some patients had a particular normal tissue improve to a greater extent than others with the JTM plan, and no correlation between improvement and parameters such as normal tissue volume or location of target was found. Studying the isodose distributions for the original and JTM plans in combination with BEVs gives an understanding of why certain structures demonstrate more of an improvement than others for a particular patient. There was also no clear parameter to identify which patients would benefit most. Integral dose generally decreased for each patient but not by a substantial margin or in a predictable manner.

Some patient structures displayed a negative response with the JTM plan indicating that the 5Gy, 10Gy or 20Gy line expanded and covered more normal tissue. This result was

unexpected as the JTM plans should be reducing MLC transmission and thus normal tissue dose. However, due to the simultaneous reduction in target dose the JTM plans had to be renormalized to maintain proper target coverage. Upon further investigation, it was found that the prescription and maximum dose (as seen in Table 3.19) of the JTM plans were much higher than that of the original plans. The increase in select normal tissue volumes receiving 5Gy, 10Gy or 20Gy was a result of the renormalization; we increased the amount of open field radiation for each segment which in some cases pushed the isodose lines to encompass more normal tissue volume. This was visually verified for each patient experiencing a negative improvement by comparing the original and JTM plan isodose lines and then viewing the BEVs. The off axis output factors in Figure 3.18 demonstrate a decrease with off axis distance on the order of our renormalization (2-3%), so this offers a plausible explanation for the renormalization.

Our measurements of MLC transmission show that Pinnacle gives a higher transmission but only a 0.2% absolute difference. The Pinnacle model for MLC transmission has a fixed value of 1.6% regardless of the MLC area exposed to primary beam while the output increases for increasing field sizes explaining the increase in transmission with decreasing field size. Our measurements showed an increase in MLC transmission with increasing field size which is expected as the larger the field size the more MLC scatter contributes to our measurement point. Pinnacle does not model MLC scatter at all, so we do not see this effect in the calculations.

The aperture measurements display higher values than Pinnacle indicating that Pinnacle underestimates phantom scatter, but by an unsubstantial amount. The difference between our measurements and Pinnacle calculations for the aperture situations was less than 0.1% and

thus uncertainties in the model did not contribute significantly to the uncertainty in the dose determination. Pinnacle models jaw and MLC transmission and scatter based on extended profiles measured at commissioning; the model gives a value for MLC and jaw transmission which may be altered in order to better match Pinnacle's model with the measured profiles. Therefore these factors in Pinnacle are essentially correction factors that increase agreement between the measured data and the model. This offers a reason why Pinnacle underestimates phantom scatter.

5   Conclusion

In this study, the linac jaws (secondary collimators) were closely collimated to the edge of each MLC aperture in step-and-shoot IMRT plans and the cumulative dose volume histogram information of the JTM plan was compared to the original clinical plans. Integral dose and maximum dose where also compared for the plans as integral dose is correlated to secondary malignancies and maximum dose quantified our increase in primary beam. Transmission measurements were also performed to validate the accuracy of using the treatment planning system Pinnacle for these dose calculations.

Ten thoracic, three head and neck and three pediatric clinically approved plans were taken and converted to plans in which each MLC aperture was surrounded by the linac jaws by a 2mm margin. This was done by making each aperture a beam and then scaling the monitor units by the appropriate collimator scatter factors to account for the change in jaw size while maintaining the original dose weighting of each segment.

We found that in general patients experienced an overall small dose reduction with the JTM plans compared to the original clinical plans. Generally the improvement in the JTM

plans was below 2%, with the greatest lung improvement in V5 and V20, 4.1% and 0.84% respectively. This means the 5 and 20Gy lines contracted with the JTM plan, reducing the lung volume covered by the 5 and 20Gy lines by 4.1% and 0.84% respectively. Integral dose generally decreased minimally for the JTM plans, typically under 2%.

Transmission through the MLC for different field sizes was measured and calculated as well as MLC and jaw transmission for an aperture situation. The results indicate that the uncertainty in Pinnacle's model did not contribute significantly to the dose determination in this research.

The hypothesis of this study was: *The volume of lung receiving 20 Gy can be reduced by greater than 10% by using the linac jaws to tightly collimate each aperture of the MLC in step-and-shoot IMRT.*

Based on the results of this study, the volume of lung receiving 20Gy cannot be reduced by greater than 10% by collimating each MLC aperture in step-and-shoot IMRT plans. Only one patient of the 16 explored experienced an improvement of that magnitude. The improvements with the JTM plans were unpredictable making it difficult to select patients that benefit the most from the jaw tracking. The JTM plans take extra time to create and our method of enabling jaw tracking will lengthen the treatment time for patients; with current Varian 2100 linear accelerators, the cost benefit ratio of clinically using this method is too high. Perhaps with the advent of new technologies such as Varian TrueBeam, that allow jaw tracking on a segment by segment basis, the clinical implementation of this method may be considered as the process will at least be somewhat easier. The results may also show more improvement with this as the jaw tracking will be included into the IMRT optimization.

6 References

1. Ferlay, J., Shin, H. R., Bray, F., Forman, D., Mathers, C. & Parkin, D. M. *Estimates of worldwide burden of cancer in 2008: GLOBOCAN 2008.* Int J Cancer.

2. Vijayakumar, S., Myrianthopoulos, L. C., Rosenberg, I., Halpern, H. J., Low, N. & Chen, G. T. *Optimization of radical radiotherapy with beam's eye view techniques for non-small cell lung cancer.* Int J Radiat Oncol Biol Phys, 1991. **21**(3): p. 779-88.

3. Chang, J.Y., H.H. Liu, and R. Komaki, *Intensity modulated radiation therapy and proton radiotherapy for non-small cell lung cancer.* Curr Oncol Rep, 2005. **7**(4): p. 255-9.

4. Liu, H.H., Wang, X., Dong, L., Wu, Q., Liao, Z., Stevens, C. W., Guerrero, T. M., Komaki, R., Cox, J. D. & Mohan, R. *Feasibility of sparing lung and other thoracic structures with intensity-modulated radiotherapy for non-small-cell lung cancer.* Int J Radiat Oncol Biol Phys, 2004. **58**(4): p. 1268-79.

5. James D. Cox, K.K.A., ed. *Radiation Oncology.* 9th ed. 2010, Mosby Elsevier. 1072.

6. Graham, M.V., Purdy, J. A., Emami, B., Harms, W., Bosch, W., Lockett, M. A. & Perez, C. A. *Clinical dose-volume histogram analysis for pneumonitis after 3D treatment for non-small cell lung cancer (NSCLC).* Int J Radiat Oncol Biol Phys, 1999. **45**(2): p. 323-9.

7. Kwa, S.L., Lebesque, J. V., Theuws, J. C., Marks, L. B., Munley, M. T., Bentel, G., Oetzel, D., Spahn, U., Graham, M. V., Drzymala, R. E., Purdy, J. A., Lichter, A. S., Martel, M. K. & Ten haken, R. K. *Radiation pneumonitis as a function of mean lung*

dose: an analysis of pooled data of 540 patients. Int J Radiat Oncol Biol Phys, 1998. **42**(1): p. 1-9.

8. Yorke, E.D., Jackson, A., Rosenzweig, K. E., Merrick, S. A., Gabrys, D., Venkatraman, E. S., Burman, C. M., Leibel, S. A. & Ling, C. C. *Dose-volume factors contributing to the incidence of radiation pneumonitis in non-small-cell lung cancer patients treated with three-dimensional conformal radiation therapy.* Int J Radiat Oncol Biol Phys, 2002. **54**(2): p. 329-39.

9. Takeda, K., Nemoto, K., Saito, H., Ogawa, Y., Takai, Y. & Yamada, S. *Dosimetric correlations of acute esophagitis in lung cancer patients treated with radiotherapy.* Int J Radiat Oncol Biol Phys, 2005. **62**(3): p. 626-9.

10. Belderbos, J., Heemsbergen, W., Hoogeman, M., Pengel, K., Rossi, M. & Lebesque, J. *Acute esophageal toxicity in non-small cell lung cancer patients after high dose conformal radiotherapy.* Radiother Oncol, 2005. **75**(2): p. 157-64.

11. Patel, A.B., Edelman, M. J., Kwok, Y., Krasna, M. J. & Suntharalingam, M. *Predictors of acute esophagitis in patients with non-small-cell lung carcinoma treated with concurrent chemotherapy and hyperfractionated radiotherapy followed by surgery.* Int J Radiat Oncol Biol Phys, 2004. **60**(4): p. 1106-12.

12. Bradley, J., Deasy, J. O., Bentzen, S. & El-Naqa, I. *Dosimetric correlates for acute esophagitis in patients treated with radiotherapy for lung carcinoma.* Int J Radiat Oncol Biol Phys, 2004. **58**(4): p. 1106-13.

13. *Diffusion Capacity.* 2010 November 3, 2010.

14. Choi, N.C. and D.J. Kanarek, *Toxicity of thoracic radiotherapy on pulmonary function in lung cancer.* Lung Cancer, 1994. **10 Suppl 1**: p. S219-30.

15.   De Jaeger, K., Seppenwoolde, Y., Boersma, L. J., Muller, S. H., Baas, P., Belderbos, J. S. & Lebesque, J. V. *Pulmonary function following high-dose radiotherapy of non-small-cell lung cancer.* Int J Radiat Oncol Biol Phys, 2003. **55**(5): p. 1331-40.

16.   Gopal, R., Starkschall, G., Tucker, S. L., Cox, J. D., Liao, Z., Hanus, M., Kelly, J. F., Stevens, C. W. & Komaki, R. *Effects of radiotherapy and chemotherapy on lung function in patients with non-small-cell lung cancer.* Int J Radiat Oncol Biol Phys, 2003. **56**(1): p. 114-20.

17.   Theuws, J.C., Kwa, S. L., Wagenaar, A. C., Seppenwoolde, Y., Boersma, L. J., Damen, E. M., Muller, S. H., Baas, P. & Lebesque, J. V. *Prediction of overall pulmonary function loss in relation to the 3-D dose distribution for patients with breast cancer and malignant lymphoma.* Radiother Oncol, 1998. **49**(3): p. 233-43.

18.   Gopal, R., *Pulmonary toxicity associated with the treatment of non-small cell lung cancer and the effects of cytoprotective strategies.* Semin Oncol, 2005. **32**(2 Suppl 3): p. S55-9.

19.   Allen, A.M., Czerminska, M., Janne, P. A., Sugarbaker, D. J., Bueno, R., Harris, J. R., Court, L. & Baldini, E. H. *Fatal pneumonitis associated with intensity-modulated radiation therapy for mesothelioma.* Int J Radiat Oncol Biol Phys, 2006. **65**(3): p. 640-5.

20.   Emami, J. Lyman, A. Brown, M.D., L. Coia, M. Goitein, J. E. Munzenrider, B. Shank, L. J. Solin**,** AND M. WESSON, *TOLERANCE OF NORMAL TISSUE TO THERAPEUTIC IRRADIATION*

Int. J. Radiation Oncology Biol. Phys., 1991. **21**: p. 109-122.

21. Mazeron, R., Etienne-Mastroianni, B., Perol, D., Arpin, D., Vincent, M., Falchero, L., Martel-Lafay, I., Carrie, C. & Claude, L. *Predictive factors of late radiation fibrosis: a prospective study in non-small cell lung cancer.* Int J Radiat Oncol Biol Phys. **77**(1): p. 38-43.

22. Hall, E.J. and C.S. Wuu, *Radiation-induced second cancers: the impact of 3D-CRT and IMRT.* Int J Radiat Oncol Biol Phys, 2003. **56**(1): p. 83-8.

23. Ruben, J.D., Lancaster, C. M., Jones, P. & Smith, R. L. *A Comparison of Out-of-Field Dose and Its Constituent Components for Intensity-Modulated Radiation Therapy Versus Conformal Radiation Therapy: Implications for Carcinogenesis.* Int J Radiat Oncol Biol Phys.

24. Kry, S.F., Salehpour, M., Followill, D. S., Stovall, M., Kuban, D. A., White, R. A. & Rosen, II *The calculated risk of fatal secondary malignancies from intensity-modulated radiation therapy.* Int J Radiat Oncol Biol Phys, 2005. **62**(4): p. 1195-203.

25. Yang, R., Xu, S., Jiang, W., Xie, C. & Wang, J. *Integral dose in three-dimensional conformal radiotherapy, intensity-modulated radiotherapy and helical tomotherapy.* Clin Oncol (R Coll Radiol), 2009. **21**(9): p. 706-12.

26. Ruben, J.D., Davis, S., Evans, C., Jones, P., Gagliardi, F., Haynes, M. & Hunter, A. *The effect of intensity-modulated radiotherapy on radiation-induced second malignancies.* Int J Radiat Oncol Biol Phys, 2008. **70**(5): p. 1530-6.

27. Khan, F.M., *The Physics of Radiation Therapy*. 4th ed. 2010: Lippincott Willimas & Wilkins.

28. Murshed, H., Liu, H. H., Liao, Z., Barker, J. L., Wang, X., Tucker, S. L., Chandra, A., Guerrero, T., Stevens, C., Chang, J. Y., Jeter, M., Cox, J. D., Komaki, R. & Mohan,

R. *Dose and volume reduction for normal lung using intensity-modulated radiotherapy for advanced-stage non-small-cell lung cancer.* Int J Radiat Oncol Biol Phys, 2004. **58**(4): p. 1258-67.

29. *American Association of Physicists in Medicine (AAPM) Report Number 72.* 2001.

30. Xia, P. and L.J. Verhey, *Delivery systems of intensity-modulated radiotherapy using conventional multileaf collimators.* Med Dosim, 2001. **26**(2): p. 169-77.

31. C. W. Taylor, P.M., S.C. Darby, *Cardiac Risks of Breast-cancer Radiotherapy: A Contemporary View.* The Royal College of Radiologists, 2006.

32. Wang, S., Liao, Z., Wei, X., Liu, H. H., Tucker, S. L., Hu, C. S., Mohan, R., Cox, J. D. & Komaki, R. *Analysis of clinical and dosimetric factors associated with treatment-related pneumonitis (TRP) in patients with non-small-cell lung cancer (NSCLC) treated with concurrent chemotherapy and three-dimensional conformal radiotherapy (3D-CRT).* Int J Radiat Oncol Biol Phys, 2006. **66**(5): p. 1399-407.

33. Lee, H.K., Vaporciyan, A. A., Cox, J. D., Tucker, S. L., Putnam, J. B., JR., Ajani, J. A., Liao, Z., Swisher, S. G., Roth, J. A., Smythe, W. R., Walsh, G. L., Mohan, R., Liu, H. H., Mooring, D. & Komaki, R. *Postoperative pulmonary complications after preoperative chemoradiation for esophageal carcinoma: correlation with pulmonary dose-volume histogram parameters.* Int J Radiat Oncol Biol Phys, 2003. **57**(5): p. 1317-22.

34. Kehwar, T.S., A.K. Bhardwaj, and S.K. Chakarvarti, *Evaluation of dosimetric effect of leaf position in a radiation field of an 80 leaf multileaf collimator fitted to the LINAC head as tertiary collimator.* J Appl Clin Med Phys, 2006. **7**(3): p. 43-54.

35. Mohan, R., Jayesh, K., Joshi, R. C., Al-Idrisi, M., Narayanamurthy, P. & Majumdar, S. K. *Dosimetric evaluation of 120-leaf multileaf collimator in a Varian linear accelerator with 6-MV and 18-MV photon beams.* J Med Phys, 2008. **33**(3): p. 114-8.

36. Prasad, S.C., *Effects of collimator jaw setting on dose output for treatments with multileaf collimator.* Med Dosim, 1998. **23**(4): p. 296-8.

37. Tobler, M., D. Leavitt, and G. Watson, *Optimization of primary jaw settings for stereotactic radiosurgery/radiotherapy.* Med Dosim, 2000. **25**(4): p. 201-8.

38. Chapek, J., Tobler, M., Toy, B. J., Lee, C. M. & Leavitt, D. D. *Optimization of collimator parameters to reduce rectal dose in intensity-modulated prostate treatment planning.* Med Dosim, 2005. **30**(4): p. 205-12.

39. Schmidhalter, D., Fix, M. K., Niederer, P., Mini, R. & Manser, P. *Leaf transmission reduction using moving jaws for dynamic MLC IMRT.* Med Phys, 2007. **34**(9): p. 3674-87.

40. Low, D.A., Harms, W. B., Mutic, S. & Purdy, J. A. *A technique for the quantitative evaluation of dose distributions.* Med Phys, 1998. **25**(5): p. 656-61.

41. Varian systems, V.m., *MLC: Systems and Maintenance Guide.*

42. Cadman, P., T. McNutt, and K. Bzdusek, *Validation of physics improvements for IMRT with a commercial treatment-planning system.* J Appl Clin Med Phys, 2005. **6**(2): p. 74-86.

43. Losasso, T., *IMRT delivery performance with a varian multileaf collimator.* Int J Radiat Oncol Biol Phys, 2008. **71**(1 Suppl): p. S85-8.

44. LoSasso, T., C.S. Chui, and C.C. Ling, *Physical and dosimetric aspects of a multileaf collimation system used in the dynamic mode for implementing intensity modulated radiotherapy.* Med Phys, 1998. **25**(10): p. 1919-27.

45. Philips, *Pinnacle Physics.* 2009. **Release 9**.

46. Philips, *Release Notes Version 9.* 2009.

47. Tailor, R., *Small field output factors.* 2011, Medical Physics.

48. Ahnesjo, A. and M.M. Aspradakis, *Dose calculations for external photon beams in radiotherapy.* Phys Med Biol, 1999. **44**(11): p. R99-155.

7 Vita

Sarah Joy was born on Offutt Air Force Base, Nebraska on October 14, 1987. After completing grade school at Lawton Chiles High School in May 2005, she entered into the University of Florida, Gainesville, Florida. She graduated Summa Cum Laude with a Bachelor of Science degree in physics in May 2009. The next two years she spent obtaining a Specialized Master of Science degree in medical physics at the University of Texas Health Science Center at Houston Graduate School of Biomedical Sciences.

Address:

7490 Brompton St. Apt 447

Houston, TX 77025